Last interglacial sea-level proxies in the Korean Peninsula

Woo Hun Ryang[1], Alexander R. Simms[2], Hyun Ho Yoon[3], Seung Soo Chun[4], and Gee Soo Kong[5]

[1] Division of Science Education and Institute of Science Education, Jeonbuk National University, Jeonju, Jeonbuk 54896, Republic of Korea

5   [2] Department of Earth Science, University of California, Santa Barbara, California 93106, U.S.A.

[3] Geological Research Division, Korea Institute of Geoscience and Mineral Resources (KIGAM), Daejeon 34132, Republic of Korea

[4] Faculty of Earth System & Environmental Sciences, Chonnam National University, Gwangju 61186, Republic of Korea

[5] Petroleum and Marine Research Division, Korea Institute of Geoscience and Mineral Resources (KIGAM), Daejeon 34132,
10   Republic of Korea

Correspondence to: Woo Hun Ryang (ryang@jbnu.ac.kr)

Abstract. Like most of the world's coastlines, the Korean Peninsula experienced higher-than-present sea levels during the Last Interglacial (LIG) otherwise known as Marine Isotope Stage (MIS) 5e. However, the expression of that highstand in sea levels differs across the eastern and western Korean Peninsula. The active east coast of the Korean Peninsula is characterized

15   by broad uplifted marine terraces, while the stable west coast is characterized by tidal flats and rias. In this study, we used a standardized database template to review and extract the existing constraints on LIG sea levels along both the east and west coasts of the Korean Peninsula. A total of 62 LIG constraining data points were compiled including 34 sea-level indicators, 22 marine limiting records, and 6 terrestrial limiting records. The ages from these data points are based on 61 optically stimulated luminescence (OSL) measurements and 1 paleomagnetic-based age. Along the uplifted east coast, LIG sea-level indicators

20   based on marine terraces are at elevations ranging from +9 to +32 m. The uplifted marine terraces are cut or otherwise deformed by faults developed under a compressional regime due to backarc closing of the East Sea since the early Pliocene. As a result, tectonic uplift likely contaminates the elevation of the east coast LIG shorelines. On the contrary, LIG sea-level constraints on the west coast of the Korean Peninsula are found at heights of between +2 and +5 m and include marine and terrestrial limiting records as well as true sea-level indicators. The LIG sea-level constraints along the west coast of the Korean Peninsula are

25   likely uncontaminated by vertical movement or experienced minor subsidence during the Quaternary.

1 Introduction

During the Last Interglacial (LIG), otherwise known as Marine Isotope Stage (MIS) 5e (about 130~115 ka), global sea level was 5~9 m higher than present sea level (Kopp et al., 2009; Dutton and Lambeck, 2012). However, the magnitude of that highstand is expressed differently across the globe depending on local tectonics, glacial-isostatic adjustment (GIA), and

30   compaction. Due to their tectonic setting, the eastern and western coasts of the Korean Peninsula record that global highstand

ca. 5 - 9 m

ca. 130 -115 ka

in sea levels differently. The eastern Korean Peninsula is tectonically active while the western Korean Peninsula has been relatively stable throughout the Quaternary (Chough et al., 2000; Chough, 2013). As a result, the active east coast of the Korean Penisula is characterized by broad uplifted marine terraces (S.J. Choi, 2019; G.Y. Lee and Park, 2019b), while the more stable west coast hosts tidal environments of its ria coast (Chough et al., 2004; Cummings et al., 2016). Available LIG constraints

35   from the east coast are based primarily on raised beach deposits overlying marine terraces, while those of the west coast are based on both presently submerged and subaerial tidal deposits. Although marine terraces are more prominent with a higher potential of preserving coastal indicators reflecting higher sea levels (Shennan et al., 2015; Rovere et al., 2016), sea-level records based on tidal deposit along the west coast may provide more valuable MIS 5e sea-level records. The value of the sea-level indicators of the western Korean Peninsula is in part due to relatively small predictions of glacial isostatic adjustment

40   (GIA) offsets across the Korean Peninsula (Creveling et al., 2017) and tectonic stability (Chough et al., 2000; Chough, 2013). In this paper, we summarize two contrasting datasets of MIS5e relative sea-level (RSL) changes from the two different tectonic settings of the eastern and western Korean Peninsula.

This work is part of the World Atlas of Last Interglacial Shorelines (WALIS) whose aim is to construct a database of LIG RSL indicators from across the globe (https://warmcoasts.eu/world-atlas.html). This paper reviews the LIG sea-level

45   constraints from the Korean Peninsula entered into the online WALIS database (zenodo). A total of 75 papers including 68 published and 7 unpublished studies were reviewed to extract 62 LIG data points comprising 34 sea-level indicators, 22 marine limiting records, and 6 terrestrial limiting records. These data are based on 61 optically stimulated luminescence (OSL) ages and 1 paleomagnetic-constraint. The database for the Korean Peninsula is available open-access in spreadsheet format as Ryang and Simms (2021), at the link: https://doi.org/10.5281/zenodo.4974826. Database field descriptions are available from

50   Rovere et al. (2020) at this link: https://doi.org/10.5281/zenodo.3961543. The following sections provide an overview of the geological and oceanographic setting of the Korean Peninsula, a history of the geological research conducted on the marine late Pleistocene deposits of the area, and an explanation of the sea-level constraints included in the database.

2 Background

2.1 Geological and Oceanographic overview

55   The tectonic framework of the Korean Peninsula reflects the large-scale interaction between the Pacific, Eurasian, and Indian plates during the Cenozoic. Two major tectonic processes govern that framework: northwestward subduction of the Pacific Plate beneath the eastern margin of the Eurasia Plate and eastward extrusion of continental crust due to the India-Eurasia collision (Molnar and Tapponnier, 1975; Watson et al., 1987; Schellart and Lister, 2005).

The East Sea (Sea of Japan) is a backarc basin on the eastern margin of the Eurasia Plate, which opened and subsided during

60   the early Oligocene through middle Miocene (32~10 Ma) (Fig. 1; Ingle, 1992; Tamaki et al., 1992; Chough et al., 2000). Since the early Pliocene (5 Ma), the sea has experienced backarc closing resulting in compressional deformation (S.H. Yoon and Chough, 1995; Kwon et al., 2009). The compressional deformation caused uplift of the eastern Korean continental margin

throughout the Quaternary (Fig. 2; Chough et al., 2000). Uplift resulted in the development of Quaternary marine terraces

along the eastern shoreline of the Korean Peninsula (Figs. 3 to 6). The marine terraces are grouped into 4 to 6 sets on the basis

65   of their elevation, ranging from 3 to 130 m above the present sea level (S.W. Kim, 1973; Oh, 1977; D.Y. Lee, 1987). Individual

terraces are overlain by 2-40 m of unconsolidated sands and well-rounded gravels (Chough et al., 2000).
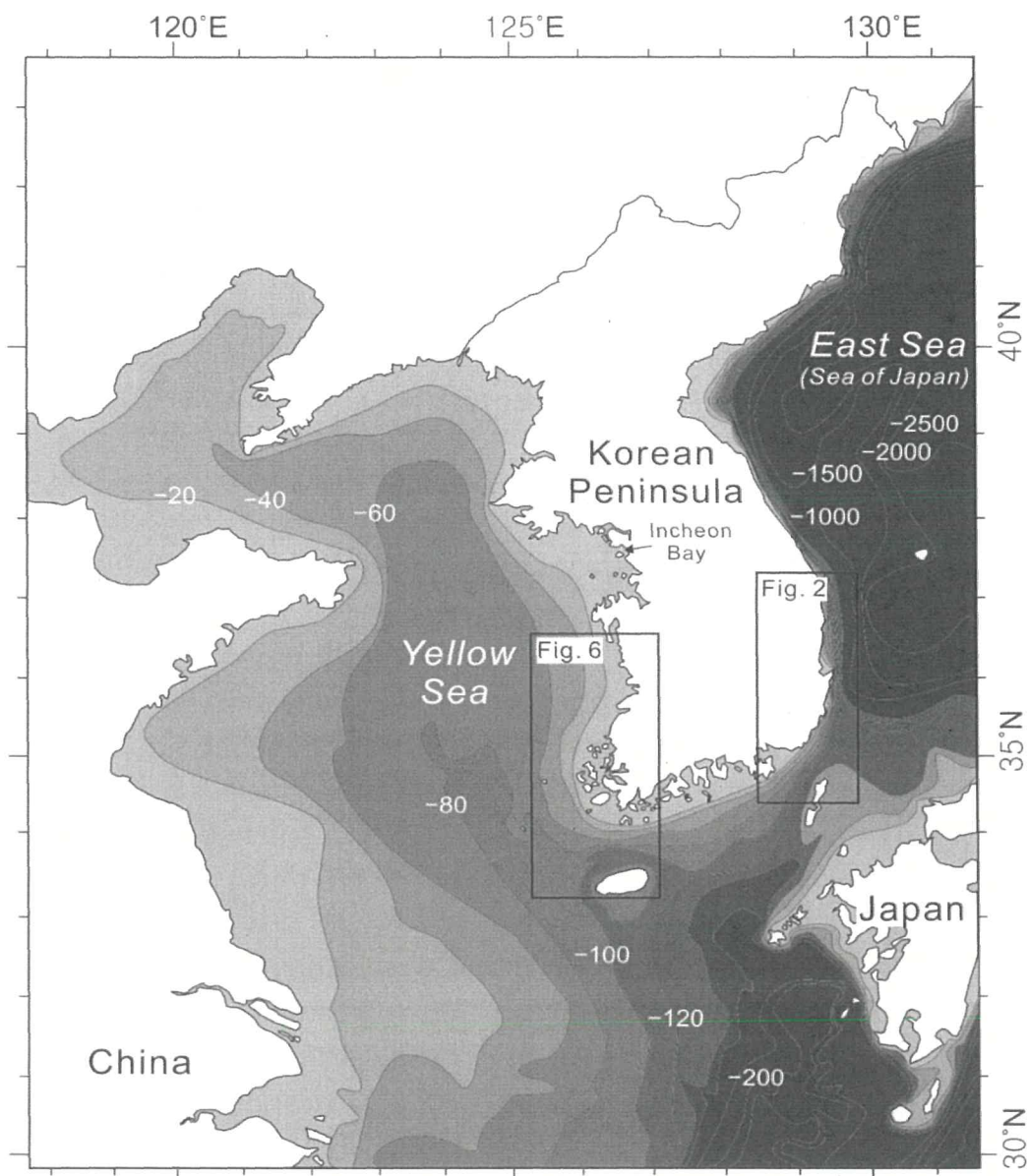
Figure 1: Bathymetry around the Korean Peninsula (modified after Chough et al., 2000; 2004; Cummings et al., 2016). Water-depth
70   **contours are in meters. Detailed maps with sampling areas are shown in Figs. 2, 7.**
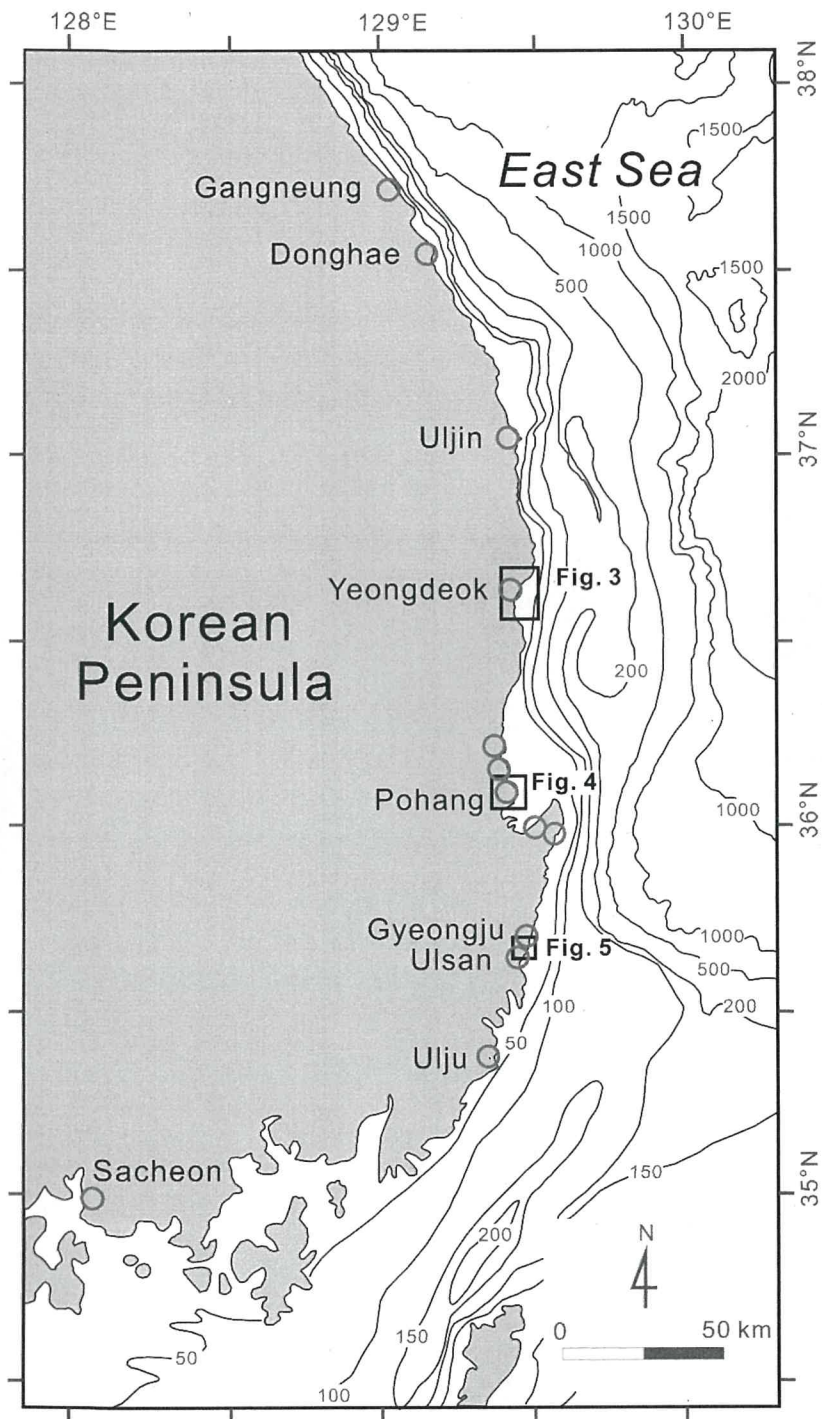
Figure 2: Map of the eastern Korean Peninsula showing detailed bathymetry and marine terraces locations. Age data are referred to in Table 3. Water-depth contours are in meters.

The East Sea is a semi-enclosed marginal sea with an average water depth of about 1350 m and a maximum water depth of about 3700 m west of the Japanese Island of Hokkaido (Chough et al., 2000). The eastern continental shelf is narrow and rapidly transitions into a deep basin (Fig. 1). Along the east coast of Korea, the tides are microtidal ranging from 10 to 30 cm, based on tide-gauges around the coast and satellite altimeter-derived (TOPEX/Poseidon) sea-surface heights (Nam et al., 2004; 2015).

The Yellow Sea is a semi-enclosed shallow epicontinental sea with an average water depth of about 55 m and a maximum depth nearing 100 m at its southeastern margin (Fig. 1; Chough et al., 2000). The seafloor of the Yellow Sea is flat and broad (Fig. 1). Based on tide-gauge observations, the tides are semidiurnal, and the tidal range varies from mesotidal (2-4 m) along the open coast to macrotidal (>4 m) within embayments (Oh and Lee, 1998; Cummings et al., 2016). Presently, high-tide beaches, multiple swash bars, cheniers, and sandy tidal-flat deposits are found along the open coast, while mud-rich tidal deposits dominate the embayed coastlines (Figs. 7, 8).

Tectonically, the Yellow Sea basins formed due to both India-Eurasia and Pacific-Eurasia plate interactions, which led to repeated extension and rifting since the Late Mesozoic (Ren et al., 2002). Extension-driven regional subsidence formed marginal basins in the Yellow Sea (Watson et al., 1987). Since the Late Miocene, the Yellow Sea is thought to have undergone little to no tectonic subsidence, and, at the least, not uplifted (Chough et al., 2000; Li et al., 2016). In the eastern Yellow Sea, the Korean Peninsula is characterized by rias and over 3000 islands along its western and southern coasts (Chough, 2013). The seafloor deepens progressively to the southeast along the NNW-SSE axis of the former Late Pleistocene lowstand shorelines (Fig. 1; Chough et al., 2000; 2004). Eustatic sea-level fluctuations during the Quaternary had a great effect on sedimentation in the Yellow Sea (Chough et al., 2000; Jin et al., 2002; Shinn et al., 2007; Yoo et al., 2016). Korean and Chinese onshore and offshore drill cores have revealed alternating terrestrial and shallow marine deposits formed during repeated Pleistocene transgressions and regressions (Li et al., 1991; Marsset et al., 1996; Jin et al., 2002; Chang et al., 2014; Li et al, 2016; S.H. Hong et al., 2019; H.H. Yoon et al., 2021). The present Yellow Sea formed during large-scale Holocene transgression of the pre-Holocene terrestrial lowlands between Korea and China (Chough et al., 2000). Many vibracores and drill cores along the west coast of Korea sample those Holocene transgressive intertidal deposits unconformably overlying the pre-Holocene semi-consolidated, oxidized floodplain deposits, forming a retrograding, coarsening-upward succession (Y.A. Park et al. 1998; Y.H. Kim et al., 1999; Lim et al. 2004; K. Choi and Kim 2006; Chang et al., 2014; H.H. Yoon et al., 2021).

2.2 Literature overview

We divided the east coast of the southern Korean Peninsula into two regions: the northern region extends from Gangneung through Uljin and to Yeongdeok (38° to 36.3°N) and the southern region extends from near Pohang to Ulju (36.3° to 35°N) (Fig. 2). Within the southern region, S.W. Kim (1973) was the first to publish ^{14}C ages from the marine terraces of Korea. He divided the marine terraces into 6 elevation groups ranging from 3 to 130 m above mean sea level (MSL) and suggested the highest two groups may have formed during a Pleistocene interglacial period. A separate study across much of the same region by G.H. Oh (1977) divided the marine terraces into 3 elevation groups ranging from 10 to 80 m above MSL. When investigating

the same region, D.Y. Lee (1987) suggested that the marine terraces were divisible into 5 elevation groups ranging from 3 m to 90 m above MSL. Based on their sedimentology and stratigraphy, D.Y. Lee (1987) suggested the highest, middle three, and lowest groups of marine terraces formed during the Pliocene, Pleistocene, and Holocene, respectively.

110
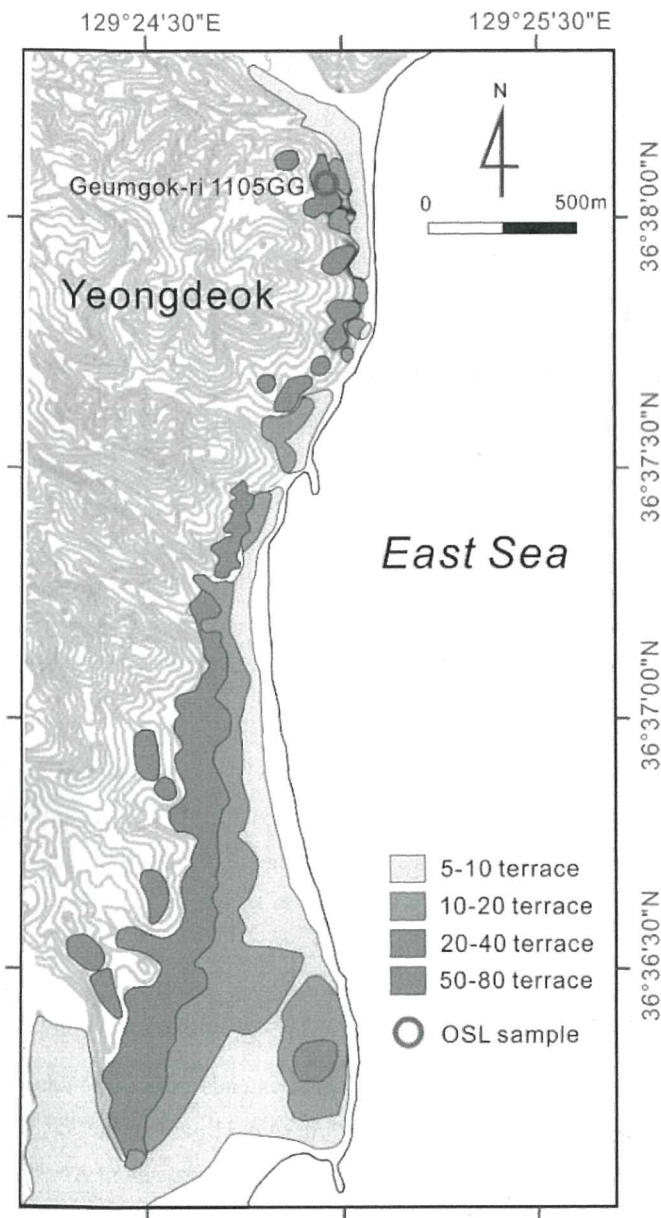
Figure 3: Marine terraces at Subsite Geumgok-ri of the Yeongdeok area in the eastern Korean Peninsula (modified after S.C. Hong, 2014). 20-40 terrace in legends indicates approximate elevations ranging from 20 to 40 m above mean sea level. For location, see Fig. 2.
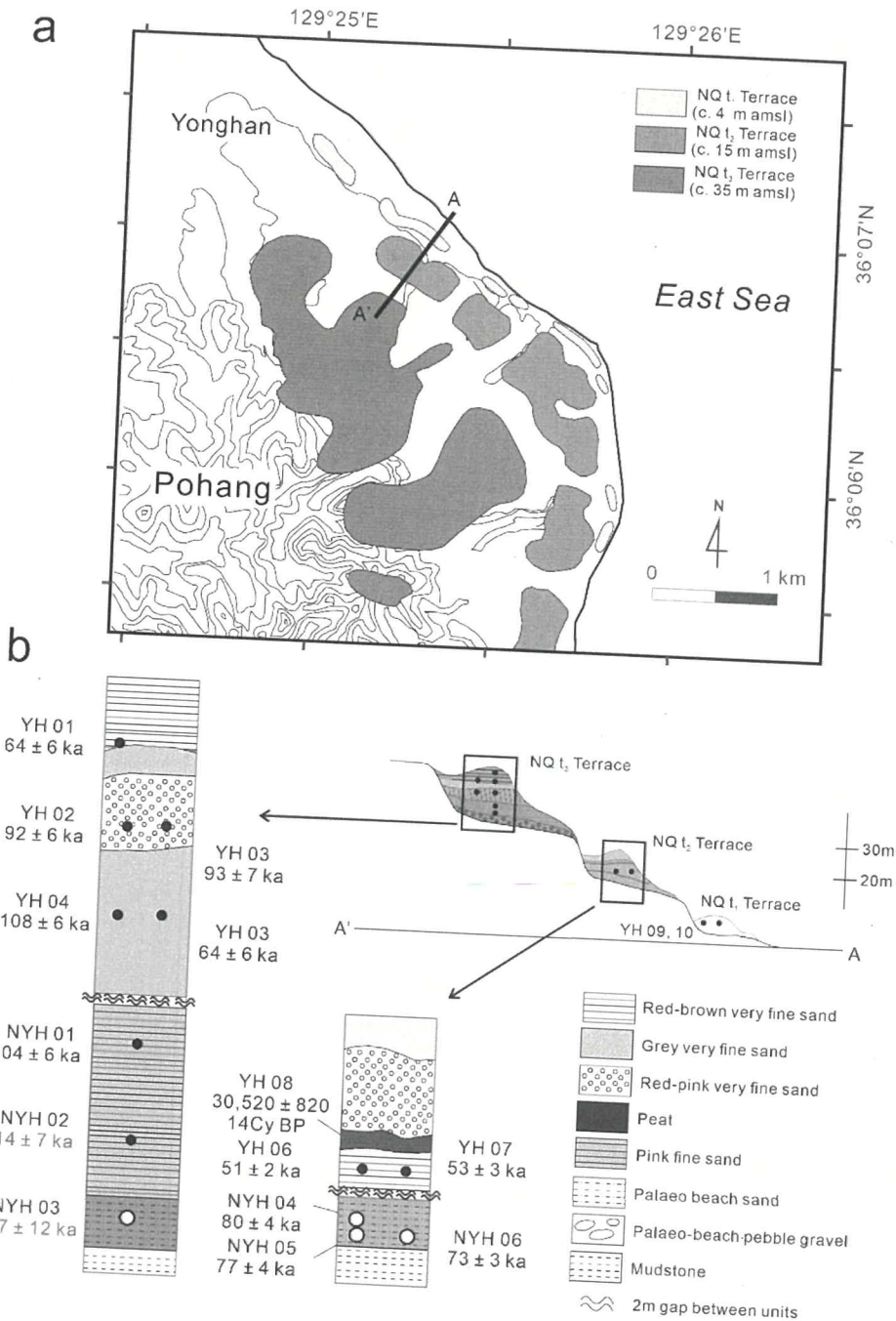
115

Figure 4: Marine terraces and columnar sections at Subsite Yonghan-2 of the Pohang area in the eastern Korean Peninsula (modified after J. H. Choi et al., 2009). (a) Plan view on the shoreline showing three group terraces. (b) Schematic cross-section and columnar sections of paleo-beach sediments overlying aeolian sand dunes on terraces. Open and closed circles indicate the samples of OSL ages from paleo-beach sediments and aeolian sand dunes, respectively. For location, see Fig. 2. amsl: above mean sea level
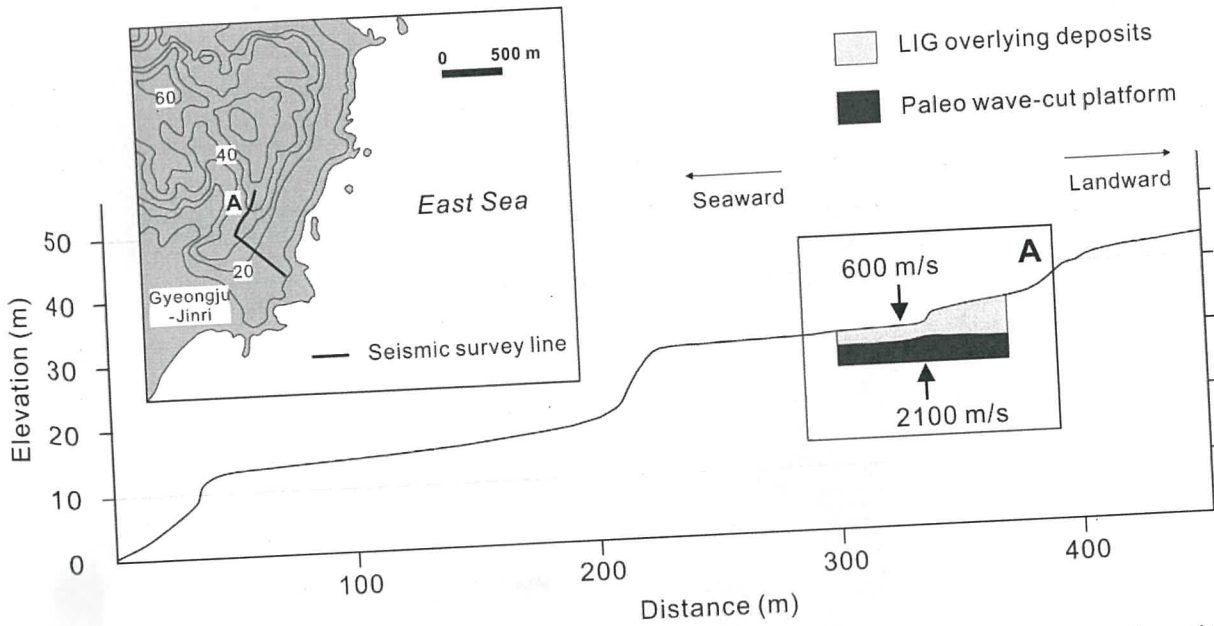
120

Figure 5: Seismic interpretation and calculated elevation of the buried LIG wave-cut platform at Subsite Jinri of the Gyeongju area, based on seismic velocities between the overlying deposits and a paleo wave-cut platform (modified after J.W. Kim et al., 2007a). For location, see Fig. 2.
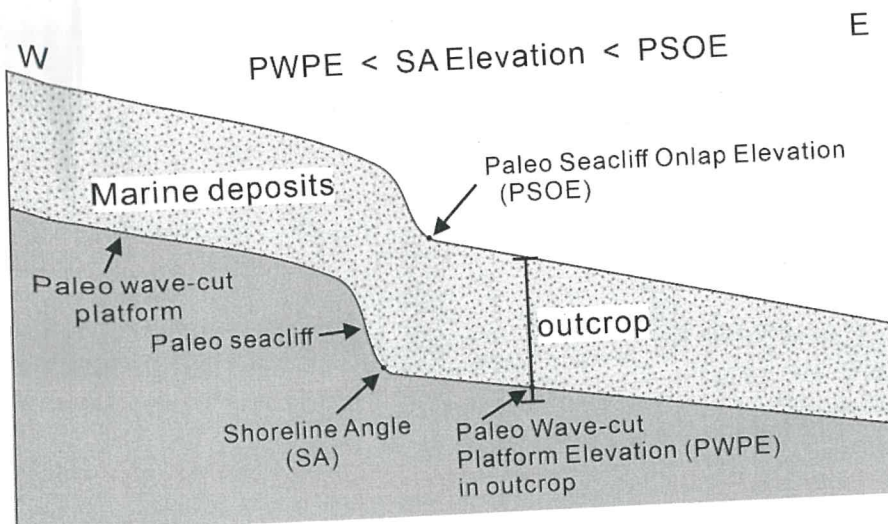
125 **Figure 6:** A schematic marine terrace commonly occurred along the eastern Korean Peninsula. Note that the shoreline angle (SA) elevation is between the paleo wave-cut platform elevation (PWPE) measured in outcrop and the paleo seacliff onlap elevation (PSOE) measured in surface topography.
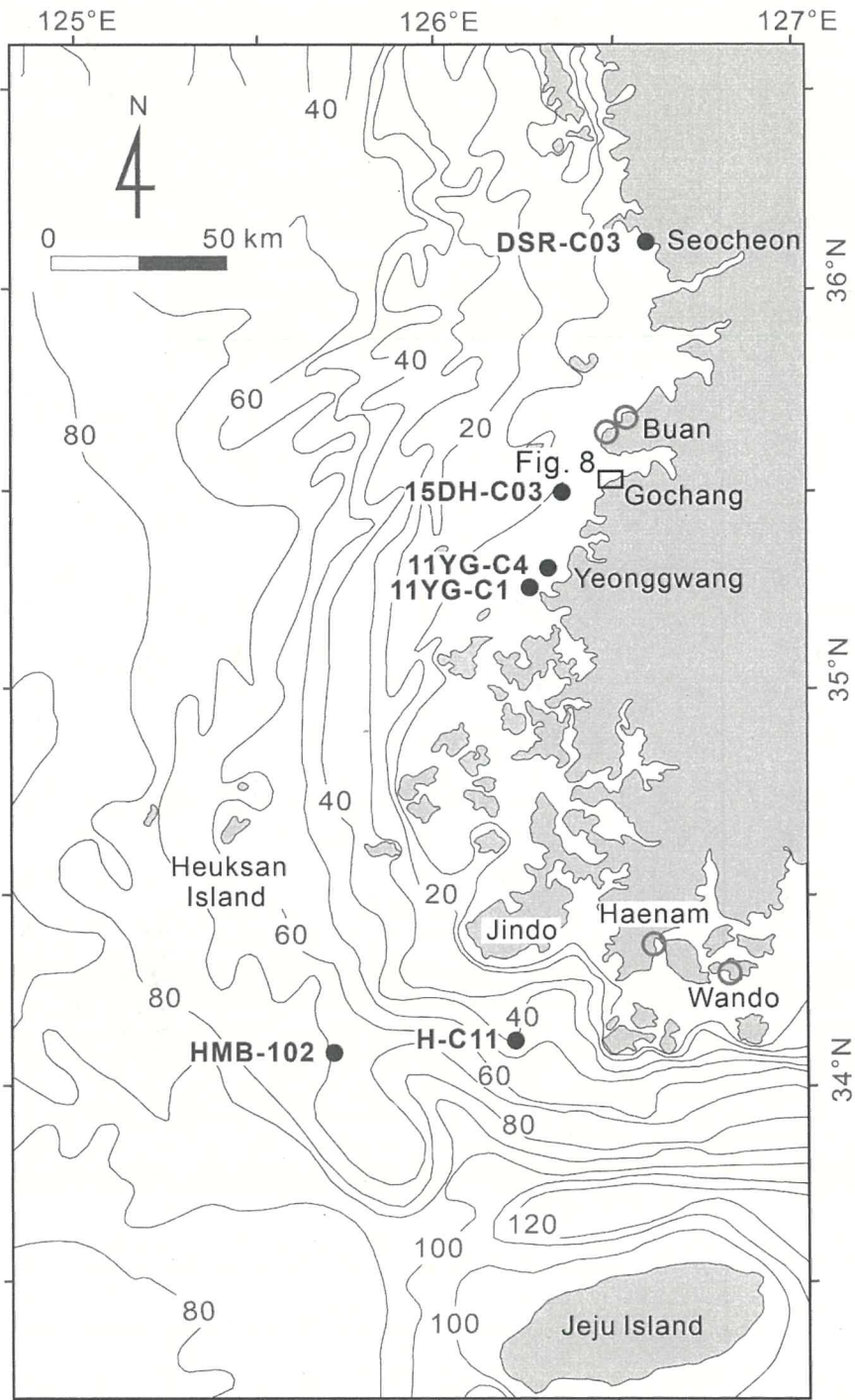
Figure 7: Location of nearshore drill cores and onshore sites. Age data are referred to in Table 3. Water-depth contours are in
130 **meters.**
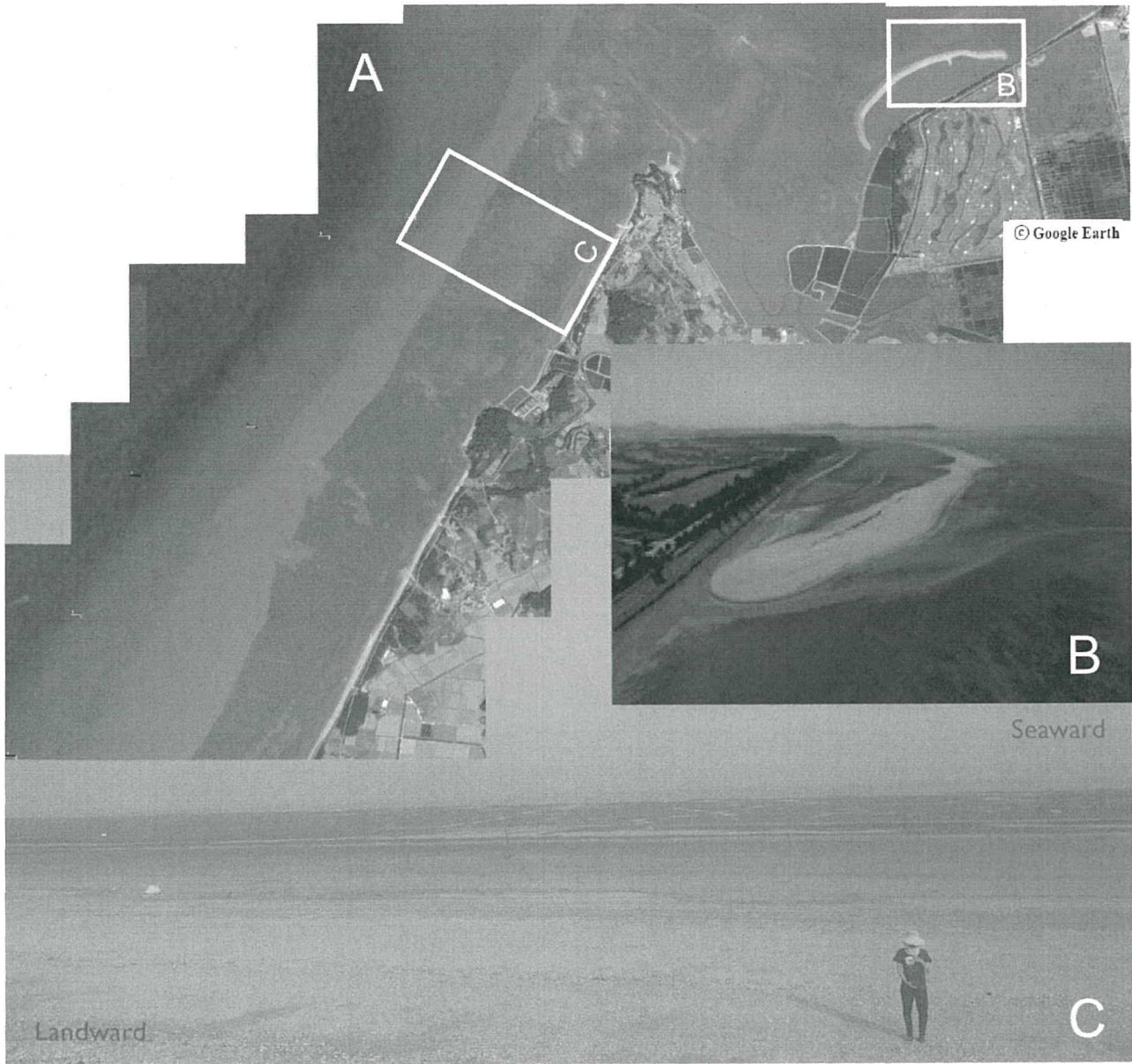
Figure 8: High-tide beaches, multiple swash bars, cheniers, and sandy tidal-flat deposits within the intertidal zone of the open coast along the western Korean coast (modified after Chun et al., 2018). (a) A satellite image with insets of landscape photographs in the Gochang area (from © Google Earth), (b) A chenier on the tidal flat (Chun et al., 2018), (c) A high-tide beach of coarse sand and middle- to low-tide intertidal flats of muddy fine sand. The sand of 2.0 ~ 3.0 Ø is predominant tending to fine seaward. For location, see Fig. 7.

In the northern region, the first LIG age (124 ka B.P.) was obtained from a fluvial terrace in the downstream part of the Seomseok river, located of Gangneung (Fig. 2), using amino acid racemization dating of peats (S.G. Choi, 1993). In the

140   southern region, another LIG age (125 ka B.P.) was obtained from a separate fluvial terrace, located near the Pohang shoreline (Fig. 2), using the same method (S.G. Choi, 1996). Since this initial work, most research has focused not on absolute age dating, but documenting the elevations, sedimentary characteristics, and stratigraphy of deposits overlying the marine terraces along the eastern shorelines (e.g., S.G. Choi, 1995a, 1995b, 2016a, 2016b, 2018, 2019; S.G. Choi and Chang, 2019; Hwang and Yoon, 1996, 2020; Hwang et al., 2012; S.O. Yoon et al., 1999, 2003, 2014).

145   In the 2000s, OSL dating started to be applied to the sandy deposits overlying the marine terraces of the eastern Korean Peninsula. The first absolute age derived by OSL dating of paleo-beach sediments overlying a marine terrace was obtained near the Ulju shoreline within the southern region (dated to 112±7 ka) (J.H. Choi et al., 2003). Other studies soon added more OSL ages of the LIG marine terraces along the east shoreline of the Korean Peninsula (J.H. Choi, 2004; J.W. Kim et al., 2005a, 2007a, 2007b; S.J. Choi et al., 2008; S.C. Hong, 2014; S.Y. Lee et al., 2015; S.J. Choi, 2016; C.S. Park et al., 2017; G.Y. Lee

150   and Park, 2019b).

Shim (2006) applied paleomagnetic analysis to outcrop sections of paleo-beach sand overlying a marine terrace along the Pohang shoreline within the southern region (Fig. 2), which was interpreted as MIS 5e deposits (114 to 120 ka). Tephrochronology and tephrostratigraphic correlation methods have also been used to suggest an MIS 5e age on deposits overlying a marine terrace at an elevation 15-20 m above MSL in the Gyeongju area of the southern region (Fig. 2; Inoue et

155   al., 2002), but the age interpretation was shortly disputed because the dated deposits may have been reworked from deposits of the higher terrace (S.J. Choi, 2003, 2009; S.J. Choi et al., 2008).

Other efforts have been underway to identify LIG marine terraces or shoreline deposits along the southern and western shorelines of the Korean Peninsula (Lee G.Y. and Park, 2006; S.G. Choi, 2006; J.H. Yang, 2008, 2011; J.H. Yang et al., 2013; S.O. Yoon et al., 2015; W.J. Shin et al., 2016; J.S. Oh, 2018; Lee G.Y. and Park, 2018). However, most of these studies relied

160   on elevation or stratigraphic correlation in the absence of absolute ages or analyzed the alluvial deposits overlying the shoreline deposits. Recently, LIG shoreline deposits were discovered on the basis of OSL ages in the Sacheon, Wando, and Haenam areas (Figs. 2, 7; D.Y. Yang et al., 2016; J.Y. Shin, 2018; G.Y. Lee and Park, 2018, 2019a; W.J. Shin et al., 2019). Arguably the best sea-level constraints from these studies are those of W.J. Shin et al. (2019). W.J. Shin et al. (2019) identified paleo-intertidal/beach deposits composed of alternating gravel and sand beds with shell fragments along the southwest Korean

165   shoreline near the Wando shoreline (Fig. 7). Their ages were obtained from intertidal/beach deposits and dated to between 115.9 ± 9.7 to 127.5 ± 8.5 ka at an elevation of 3.5 to 2.8 m above MSL (W.J. Shin et al., 2019).

3 Methods

3.1 Elevation details

3.1.1 Datums

Earth System
Science
Data

170 The Korean geodetic horizontal point is based on the World Geodetic Reference System (ITRF2000 & GRS80). This horizontal and vertical datum has been well managed for the national territory by the National Geographic Information Institute (2021). The Korean official vertical datum is based on mean sea level within Incheon Bay from 1913 to 1916 (Fig. 1). Using the datum, the institute installed a series of nationally unified control points and benchmarks across the entire Korean peninsula and territorial islands. All elevation data in this paper were measured using this national geodetic system.

175 **3.1.2 Elevation measurements**

All surveys include GPS or DGPS surveying methods. Most surveys also used an electro-optical distance measuring system (total station) to determine the elevation at specific points from a local benchmark of the Korean official vertical datum. Some locations were determined by comparing the GPS coordinates of the sampling point with a 1:5000 topographic map. Marine surveys used a virtual reference station linked to a GPS (VRS-GPS) or DGPS and a high-resolution echosounder aboard the

180 drilling ship.

3.2 Coring

Cores were acquired using a hydraulic-powered drill on a barge or a ship-deployed vibrocorer. Sediment sampling was performed using a standard thin-walled 55-mm diameter tube sampler. In the laboratory, cores were split lengthwise, described, photographed, and sampled. Core descriptions were based on sediment characteristics, including color, lithology, texture, grain

185 size, and structure. *any faunal elements?*

3.3 Dating techniques

3.3.1 Optically stimulated luminescence

Sixty-one of the 62 absolute ages in this dataset were acquired using OSL. Fifty-one OSL dating measurements were conducted on coarse-grained sand or fine-grained silt quartz separates. Seven additional ages were obtained from K-feldspar minerals (IRSL, Infrared Stimulated Luminescence) isolated from coarse-grained sand and another 3 ages were obtained from K-

190 feldspar minerals of gravel surfaces (rock surface OSL dating) (e.g., J.H. Choi et al., 2004; S.C. Hong et al., 2013; S.C. Hong, 2014, 2016). All OSL ages were conducted using the single-aliquot regenerative-dose (SAR) procedure (Murray and Wintle 2000).

3.3.2 Paleomagnetism

195 For the paleomagnetic study, sediment samples were collected almost continuously from an outcrop using non-magnetic 22 × 22 × 22 mm³ plastic cubes. The remanent magnetic moment of each sample was measured by a high-temperature superconducting magnetometer (F.I.T Messtechnik GmbH, HSM2) at Hanyang University (Shim, 2006). Alternating field demagnetization (Molspin Co.) and anhysteric/isothermal remanent magnetization experiments were performed to isolate the

What about the Amino Rasinsation?

characteristic remanent magnetization of each sample (Shim, 2006). Magnetic susceptibility was measured by a susceptibility
200   meter (Bartington Co., MS2F) for determining the types and amounts of ferrimagnetic minerals in the sediments.

3.3.3 Relative sea-level elevation assignments

3.3.3.1 Paleo sea level from marine terraces

The approach used to reconstruct paleo RSLs is in part dependent on the landform used (Tables 1, 2). The most commonly
applied approach to reconstructing past RSLs from marine terraces is to use the elevation of the shoreline angle (SA in Fig. 6;
205   "inner edge" of Bradley and Griggs, 1976) or junction between the marine platform and the paleo sea cliff of Muhs et al., 1990)
as a proxy for paleo sea levels. Unfortunately for most of the data collected to date across the marine terraces of the east coast
of the Korean Peninsula, the shoreline angle (SA) elevation is unknown because the paleo-sea cliffs are covered by overlying
deposits (Fig. 6). Only 3 shoreline angle elevations, representing 3 of the 13 subsites, were measured in the original studies
(Table 2; Fig. 5). In the case of an unknown shoreline angle elevation but where a paleo wave-cut platform elevation (PWPE)
210   and a paleo seacliff onlap elevation (PSOE) were measured (Table 2; Fig. 6), we expressed the estimated shoreline angle
elevation (SA_e) as the mid-point elevation between the PWPE and the PSOE with an error range (δ_{SAe}) of ½ that elevation
difference according to the following equations:

$$SA_e = \frac{(PSOE + PWPE)}{2} \tag{1}$$

$$\delta_{SAe} = \frac{(PSOE - PWPE)}{2} \tag{2}.$$

215   This approach allowed us to estimate RSLs from two additional subsites where the PWPE and the PSOE are measured in the
field (Table 2; Fig. 6).

RSL is where calculated from all sea-level indicators using the following equations:

$$\text{Paleo RSL} = E - RWL \pm \frac{\delta_{RSL}}{2} \tag{3}$$

where E, RWL, and δ_{RSL} represent a measured elevation of sea-level indicator in the field, a reference water level for the
220   respective sea-level indicator, and an uncertainty in paleo RSL, respectively (Rovere et al., 2016).

$$RWL = \frac{U_l + L_l}{2} = \frac{SWSH + d_b}{2} \tag{4}$$

where U_l, L_l, SWSH, and d_b represent the upper limit of the modern analogue landform's elevation and the lower limit of the
modern analogue landform's elevation. These latter two are equivalent to the storm wave swash height and a breaking depth,
respectively in the case of most sea-level indicator used in this study (Table 1; Rovere et al., 2016). Breaking depth was
225   approximated using the following equation:

$$d_b = -\frac{H_s}{0.78} \tag{5}$$

where H_s represents an average significant wave height during one year and 0.78 is commonly used for wave breaking criteria
on a smooth, flat slope (Table 1; U.S. Army Corps of Engineers, 1984; Rovere et al., 2016).

$$\delta_{RSL} = \sqrt{E_e^2 + \left(\frac{IR}{2}\right)^2} = \sqrt{E_e^2 + \left(\frac{U_l - L_l}{2}\right)^2} = \sqrt{E_e^2 + \left(\frac{SWSH - d_b}{2}\right)^2} \qquad (6)$$

230   where E_e and IR represent an error in the elevation measurement (standard deviation) and the indicative range, respectively (Rovere et al., 2016). For the case of marine terraces whose shoreline angle was measured or estimated, their RSL equivalent (Paleo SA RSL) would be:

$$\text{Paleo SA RSL} = \frac{PSOE + PWPE}{2} - RWL \pm \left(\frac{\delta_{RSL}}{2} + \frac{PSOE - PWPE}{2}\right) \qquad (7).$$

The storm wave swash height (SWSH), average significant wave heights (H_s), and breaking depths (d_b) were obtained from

235   local sources (Table 2).

In cases along the east coast of the Korean Peninsula where both the elevation of the shoreline angle or paleo wave-cut platform are unknown, we base our estimates of RSL by treating the dated deposits overlying the marine terraces as beach sands using Eq. 8.

Paleo RSL at marine-terrace data points (Landform Type 1 in Table 1)

240   $$= E - RWL \pm \sqrt{E_e^2 + \left(\frac{SWSH - d_b}{2}\right)^2} \qquad (8).$$

We used local storm wave swash height (SWSH), average significant wave heights (H_s), and breaking depths (d_b) to calculate 30 paleo RSLs from the elevations of the beach sands overlying the marine terraces along the east coast (Table 3).

245   Table 1. Landforms used for calculating paleo relative sea level in this study.

Type	Landform	Upper limit	Lower limit	Definitions and Data
1	Beach sands overlying marine terraces ("marine terraces" of Rovere et al., 2016)	Storm Wave Swash Height (SWSH)	Breaking depth (d_b)	**MHHW**: mean higher high water, the average of the higher high water height of each tidal day (Pugh and Woodworth, 2014)
				MLLW: mean lower low water, the average of the lower low water height of each tidal day (Pugh and Woodworth, 2014)
2	Beach deposits (Rovere et al., 2016)	Ordinary berm (ob)	Breaking depth (d_b)	This study used the average heights of statistically estimated MHHW and MLLW of each tidal day observed during January, February, and March 2021 in the nearest station from the shoreline at each subsite (KHOA, 2021)
3	Beach rock (Rovere et al., 2016)	Spray zone (sz)	Breaking depth (d_b)	**SWSH**: storm wave swash height, the maximum elevation reached by extreme storms on the beach (Otvos, 2000)
4	Tidal-flat clastic deposits	Spray zone (sz)	Sum of mean lower low water and breaking depth (MLLW + d_b)	**H$_s$**: average significant wave height during one year (U.S. Army Corps of Engineers, 1984)
				This study used the maximum wave height for SWSH and average significant wave height for H_s observed during 2020 in the nearest station from the shoreline at each subsite (KHOA, 2021).
				d_b: breaking depth, for a smooth, flat slope, $d_b = - H_s/0.78$ (U.S. Army Corps of Engineers, 1984)
				ob: ordinary berm height, ob = 0.2 x H_s + MHHW (Mayer and Kriebel, 1994)
				sz: spray zone height, sz = 2 x ob (Rovere et al., 2016)

Table 2. Summary of LIG relative sea level of the shoreline angle along the East Coast of the Korean Peninsula.

No.	Site	Subsite	Sample latitude (°)	Sample longitude (°)	Landform Type in Table 1	LIG RSL at the shoreline angle (m)	± Error of LIG RSL (m)	Measured elevation of the shoreline angle (m)	Measured elevation of paleo wave-cut platform (PWPE) (m)	Measured elevation of paleo seacliff onlap (PSOE) (m)	Topographic elevation range of paleo-shoreline deposits (m)	Reference
1	Gangneung	Anin	37.7401	128.9716	1	22.2	2.2	25.0	21.4	30	20~30	S.Y. Lee et al., 2015
2	Pohang	Yonghan-2	36.1085	129.4230	1	33.2	1.7	35.0	34.4	?	?	J.H. Choi et al., 2009
3	Gyeongju	Jinri	35.6827	129.4686	1	25.0	2.5	29.0	29.0	45	30~45	J.W. Kim et al., 2007a
4	Donghae	Eodal-dong	37.5657	129.1181	1	27.7	6.7	?	26.0	35	25~35	S.C. Hong, 2014
5	Pohang	Masan-ri	36.0152	129.4826	1	21.7	3.2	?	22.0	25	10~25	J.W. Kim et al., 2005b
Table 3. Summary of LIG relative sea levels and ages as data points in the Korean Peninsula. For references, refer to the text. SLI:
250 **sea level indicator; TL: terrestrial limiting record; ML: marine limiting record.**

WALIS LUM ID	Site	Subsite	Sample latitude (°)	Sample longitude (°)	Indicator Type	Landform type in Table 1	Paleo RSL (m)	± Error of paleo RSL	Elevation above MSL (m)	Dating method	OSL mineral type	Age (ka)	± Age uncertainty (ka)
432	Gang neung	Saemok ee	37.7402	128.9716	SLI	1	26.9	2.2	29.7	OSL	K-Feldspar	128.3	24.5
433	Gang neung	Saemok ee	37.7402	128.9716	SLI	1	26.9	2.2	29.7	OSL	K-Feldspar	124.1	25.3
434	Gang neung	Saemok ee surface age	37.7402	128.9716	SLI	1	25.9	2.2	28.7	OSL	K-Feldspar (gravel surface)	133.7	13.9
435	Gang neung	Anin	37.7401	128.9716	SLI	1	20.3	2.2	23.08	OSL	Quartz	117.0	6.0
436	Gang neung	Anin	37.7401	128.9716	SLI	1	20.3	2.2	23.09	OSL	Quartz	129.0	8.0
492	Dong hae	Eodal-dong 1	37.5657	129.1181	SLI	1	27.4	2.2	30.2	OSL	Quartz	126.1	10.1
437	Dong hae	Eodal-dong 1	37.5657	129.1181	SLI	1	27.4	2.2	30.2	OSL	K-Feldspar	127.5	24.6
438	Dong hae	Eodal-dong 2	37.5657	129.1181	SLI	1	26.4	2.2	29.2	OSL	Quartz	128.0	14.0
439	Dong hae	Eodal-dong 2	37.5657	129.1181	SLI	1	26.4	2.2	29.2	OSL	K-Feldspar	124.1	23.7
440	Dong hae	Eodal-dong 3	37.5657	129.1181	SLI	1	25.4	2.2	28.2	OSL	Quartz	112.1	7.7
441	Dong hae	Eodal-dong 3	37.5657	129.1181	SLI	1	25.4	2.2	28.2	OSL	K-Feldspar	125.3	24.0
442	Uljin	Hujeong 1 (Gwang yoon Apt.)	37.0619	129.4153	SLI	1	28.2	1.7	30	OSL	Quartz	119.0	15.0
443	Uljin	Hujeong 2 (Gwang yoon Apt.)	37.0619	129.4153	SLI	1	32.2	1.7	34	OSL	Quartz	111.0	9.0
444	Yeon gdeok	Geumgo k-ri 1	36.6362	129.4150	SLI	1	19.4	1.7	21.2	OSL	K-Feldspar	124.5	25.3
445	Yeon gdeok	Geumgo k-ri 2	36.6362	129.4150	SLI	1	22.1	1.7	23.9	OSL	K-Feldspar	122.1	24.9

446	Pohang	Josa-ri	36.2194	129.3801	SLI	1	20.2	1.7	22	OSL	Quartz	116.0	8.0
447	Pohang	Ohdo-ri	36.1586	129.3969	SLI	1	23.4	1.7	25.23	OSL	Quartz	137.0	9.0
448	Pohang	Yonghan-1 (silica mine)	36.1093	129.4161	SLI	1	30.2	1.7	32	OSL	Quartz	123.0	9.0
449	Pohang	Yonghan-2a	36.1085	129.4230	TL	1	33.7	1.7	35.5	OSL	Quartz	114.0	7.0
450	Pohang	Yonghan-2b	36.1085	129.4230	SLI	1	33.2	1.7	35	OSL	Quartz	127.0	12.0
451	Pohang	Masan-ri	36.0152	129.4826	SLI	1	21.2	1.7	23	OSL	Quartz	119.0	8.0
452	Pohang	Masan-ri	36.0152	129.4826	SLI	1	21.7	1.7	23.5	OSL	Quartz	111.0	5.0
453	Pohang	Masan-ri	36.0152	129.4826	SLI	1	22.2	1.7	24	OSL	Quartz	116.0	7.0
454	Pohang	Masan-ri	36.0152	129.4826	SLI	1	22.7	1.7	24.5	OSL	Quartz	107.0	8.0
–	Pohang	Masan-ri	36.0152	129.4826	SLI	1	21.2	1.7	23	Paleomagnetism	–	117.6	2.7
455	Pohang	Hajeong-ri	35.9716	129.5493	TL	1	33.2	1.7	35	OSL	Quartz	128.0	12.0
456	Gyeongju	Jinri	35.6827	129.4686	SLI	1	32.3	2.6	36	OSL	Quartz	116.0	6.0
457	Gyeongju	Jinri	35.6827	129.4686	SLI	1	32.3	2.6	36	OSL	Quartz	126.0	10.0
459	Ulsan	Jeongja-ri	35.6311	129.4331	SLI	1	18.8	2.6	22.5	OSL	Quartz	113.0	39.0
458	Ulju	Weseong	35.3821	129.3414	SLI	1	10.3	2.6	14	OSL	Quartz	112.0	7.0
460	Sacheon	Daepo-dong	34.9900	128.0427	SLI	2	6.0	0.8	6	OSL	K-Feldspar (cobble surface)	111.2	16.0
461	Sacheon	Daepo-dong	34.9900	128.0427	SLI	2	6.0	0.8	6	OSL	K-Feldspar (cobble surface)	102.5	14.7
462	Wando	Sinji 1	34.3258	126.8286	SLI	2	2.5	0.9	2.8	OSL	Quartz	127.5	8.5
463	Wando	Sinji 1	34.3258	126.8286	SLI	2	3.2	0.9	3.5	OSL	Quartz	115.9	9.7

464	Wando	Sinji 3	34.3280	126.8258	SLI	2	5.8	0.9	6.1	OSL	Quartz	108.0	18.0
465	Haenam	Ijin-ri 1	34.3962	126.6175	TL	3	6.4	1.3	7.51	OSL	Quartz	121.0	10.0
466	Haenam	Ijin-ri 2	34.3962	126.6175	TL	3	5.3	1.3	6.49	OSL	Quartz	128.0	10.0
467	Haenam	Ijin-ri 3	34.3962	126.6175	TL	3	4.3	1.3	5.41	OSL	Quartz	128.0	9.0
468	Buan	Daehang-ri	35.6790	126.5312	TL	3	8.2	2.0	10.78	OSL	Quartz	112.0	24.0
469	Buan	Mapo-ri	35.6523	126.5073	TL	3	6.2	2.0	8.8	OSL	Quartz	130.0	20.0
470	Seocheon	Dasa-ri 1	36.1043	126.6078	ML	4	-3.8	2.5	-1.88	OSL	Quartz	116.0	10.0
471	Seocheon	Dasa-ri 2	36.1043	126.6078	ML	4	-5.7	2.5	-3.82	OSL	Quartz	108.0	8.0
472	Yeonggwang	Baeksu 1	35.3032	126.3212	ML	4	-22.8	2.5	-20.8	OSL	Quartz	110.0	6.6
473	Yeonggwang	Baeksu 2	35.3032	126.3212	ML	4	-24.1	2.5	-22.1	OSL	Quartz	133.9	7.6
474	Yeonggwang	Baeksu 3	35.3032	126.3212	ML	4	-25.9	2.5	-23.9	OSL	Quartz	124.0	7.8
475	Yeonggwang	Baeksu 4	35.3032	126.3212	ML	4	-27.2	2.5	-25.2	OSL	Quartz	138.8	7.8
476	Yeonggwang	Baeksu 5	35.3032	126.3212	ML	4	-28.8	2.5	-26.8	OSL	Quartz	128.7	7.9
477	Yeonggwang	Baeksu 6	35.3032	126.3212	ML	4	-30.3	2.5	-28.3	OSL	Quartz	124.7	7.6
478	Yeonggwang	Baeksu 7	35.3032	126.3212	ML	4	-31.8	2.5	-29.8	OSL	Quartz	118.8	7.0
479	Yeonggwang	Baeksu 8	35.3032	126.3212	ML	4	-33.3	2.5	-31.3	OSL	Quartz	112.2	6.8
480	Yeonggwang	Baeksu 9	35.3032	126.3212	ML	4	-34.8	2.5	-32.8	OSL	Quartz	113.4	7.1

481	Yeon ggwa ng	Baeksu 10	35.3032	126.3212	ML	4	-36.3	2.5	-34.3	OSL	Quartz	118.2	7.4
482	Yeon ggwa ng	Baeksu 11	35.3032	126.3212	ML	4	-37.8	2.5	-35.8	OSL	Quartz	112.6	6.9
483	Yeon ggwa ng	Baeksu 12	35.3032	126.3212	ML	4	-39.3	2.5	-37.3	OSL	Quartz	113.1	7.3
484	Yeon ggwa ng	Baeksu-Duuri 1	35.2723	126.2845	ML	4	-17.4	2.5	-15.48	OSL	Quartz	107.7	6.7
485	Yeon ggwa ng	Baeksu-Duuri 2	35.2723	126.2845	ML	4	-27.9	2.5	-25.98	OSL	Quartz	122.1	7.2
486	Yeon ggwa ng	Baeksu-Duuri 3	35.2723	126.2845	ML	4	-29.2	2.5	-27.28	OSL	Quartz	126.2	8.1
487	Gocha ng	Dongho 1	35.4911	126.3678	ML	4	-37.2	2.5	-35.2	OSL	Quartz	107.5	7.6
488	Gocha ng	Dongho 2	35.4911	126.3678	ML	4	-39.4	2.5	-37.4	OSL	Quartz	107.6	7.3
489	Gocha ng	Dongho 3	35.4911	126.3678	ML	4	-40.2	2.5	-38.2	OSL	Quartz	113.3	7.2
490	Jindo	Jindo shelf	34.1205	126.2188	ML	4	-49.0	1.5	-48.5	OSL	Quartz	124.4	10.0
491	Heuks an Island	Heuksan Mud Belt	34.1326	125.6823	ML	4	-84.7	1.6	-84	OSL	Quartz	125.1	9.9

3.3.3.2 Paleo sea level calculated from beach and tidal deposits

Beach deposits and beach rock are also a reliable RSL marker because the formative zone is in close relation to sea levels (Mauz et al., 2015). Five paleo RSLs of beach deposits (Landform Type 2 in Table 1) and an additional five paleo RSLs of
255 beach rock (Landform Type 3 in Table 1) were used to determine paleo RSLs from LIG-aged deposits along the western and southern Korean coast. RSLs from beach rock were calculated using the following equations:

Paleo RSL at beach-deposit data points (Landform Type 2 in Table 1)

$$= E - RWL \pm \sqrt{E_e^2 + \left(\frac{ob - d_b}{2}\right)^2} = \sqrt{E_e^2 + \left(\frac{(0.2 * H_s + MHHW) - d_b}{2}\right)^2} \qquad (9)$$

where (ob) represents the ordinary berm height, which was estimated using the average significant wave height over one year
260 (H_s) and MHHW represents the mean higher high water heights (Table 1; Mayer and Kriebel, 1994; Rovere et al., 2016). For beach rocks, we used a similar expression:

Paleo RSL at beach-rock data points (Landform Type 3 in Table 1)

$$= E - RWL \pm \sqrt{E_e^2 + \left(\frac{sz - d_b}{2}\right)^2} = \sqrt{E_e^2 + \left(\frac{2*(0.2*H_s + MHHW) - d_b}{2}\right)^2} \qquad (10)$$

where (sz) represents the elevation of the top of the spray zone, which was calculated using the average significant wave height over one year (H_s) (Table 1; Rovere et al., 2016).

Twenty-two OSL-dated clastic tidal-flat deposits from nearshore cores were also used to estimate paleo RSLs based on Eq. (11).

Paleo RSL at tidal-flat clastic data points (Landform Type 4 in Table 1)

$$= E - RWL \pm \sqrt{E_e^2 + \left(\frac{sz - (MLLW + d_b)}{2}\right)^2} = \sqrt{E_e^2 + \left(\frac{2*(0.2*H_s + MHHW) - (MLLW + d_b)}{2}\right)^2} \qquad (11)$$

where MLLW represents mean lower low water heights (Table 1).

4 Relative Sea-level Indicators

In the following sections, we discuss each characteristic of the RSL indicators from the Korean Peninsula, identified by thier 'WALIS RSL ID' in the text, that have been entered into the WALIS database. The ID number corresponds with the WALIS database identification numbers. Similarly, we use 'WALIS LUM ID' followed by a number to reference an optically stimulated luminescence (LUM) age within the database.

The east coast of the southern Korean Peninsula was divided into two regions, a northern and a southern region, based on latitude. The northern region encompasses the area from Gangneung through Uljin and the Yeongdeok area (38°N to 36.3°N) while the southern region encompasses the region between Pohang and Ulsan (36.3°N to 35°N) (Fig. 2). Along the west and southwest coast of the southern Korean Peninsula, the sea-level data and indicators were divided into two groups, those found onshore and those found within the nearshore.

4.1 Marine terraces along the northern east coast

4.1.1 Gangneung area

Two areas have been studied within the Gangneung area: Gangneung-Saemokee and Gangneung-Anin (Fig. 2). The marine deposits overlying the paleo wave-cut platform of the marine terrace at Gangneung-Saemokee are found 27~31 m above MSL and contain rounded cobbles and some sand deposits of paleo-beach origin (S.C. Hong, 2014). At Subsite Gangneung-Saemokee, two quartz OSL ages were interpreted as minimum ages of >85 ka and >92 ka. These deposits appear to exceed the upper age limit of the methodology because the signal is saturated (e.g., Rhodes, 2011). Fortunately, two IRSL ages of 128.3±24.5 ka (WALIS LUM ID #432) and 124.1±25.3 ka (WALIS LUM ID #433) and one cobble surface OSL age of 133.7±13.9 ka (WALIS LUM ID #434) were obtained from these terrace deposits (Table 3; S.C. Hong, 2014). Using Eq. (8),

290 the paleo RSLs of these samples without a PWPE yielded 26.9±2.2 m, 26.9±2.2 m, and 25.9±2.2 m above MSL, respectively (Table 3; WALIS RSL ID #4009, 4010).

Gangneung-Anin is located 23 m above MSL and consists of beach sand and gravel deposits overlying a paleo wave-cut platform. The two ages from the beach sand were 117±6 ka (WALIS LUM ID #435) and 129±8 ka (WALIS LUM ID #436) (Table 3; S.Y. Lee et al., 2015). Using Eq. (8), the paleo RSLs of these samples without a PWPE yielded 20.3±2,2 m above

295 MSL (Table 3; WALIS RSL ID #4011). In this area, the elevation of the LIG shoreline angle is 25 m above MSL (Lee et al., 2015). The LIG RSL based on this shoreline angle elevation is 22.2 ±2.2 m above MSL when using Eq. (7) (Table 2).

4.1.2 Donghae area

Donghae-Eodal-dong is located 26 m above MSL (Fig. 2) and consists of beach sand and pebble deposits overlying a paleo wave-cut platform. The three samples from the beach sand were analyzed using paired OSL and IRSL methods. The three

300 OSL/IRSL age sets from the beach sand were 126.1±10.1 ka (OSL, WALIS LUM ID #492) and 127.5±24.6 ka (IRSL, WALIS LUM ID #437), 128±14 ka (OSL, WALIS LUM ID #438) and 124.1±23.7 ka (IRSL, WALIS LUM ID #439), and 112.1±7.7 ka (OSL, WALIS LUM ID #440) and 125.3±24 ka (IRSL, WALIS LUM ID #441) (Table 3; S.C. Hong, 2014). Using Eq. (8), the paleo RSLs of these samples without a PWPE yielded 27.4±2.2 m, 26.4±2.2 m, and 25.4±2.2 m above MSL, respectively (Table 3; WALIS RSL ID #4012, 4014, 4015). At this site, the elevation of the paleo wave-cut platform is 26.0 m above MSL.

305 Although the paleo shoreline angle elevation is unknown, we estimated the paleo shoreline angle RSL to be approximately 27.7±6.7 m above MSL using Eq. (7) with 26 m PWPE and 35 m PSOE (Table 2).

4.1.3 Uljin area

Subsite Uljin-Hujeong is located 30~34 m above MSL (Fig. 2) and is comprised of moderately well-sorted sand (>5 m thick) with a mean grain size of ~ 1.3 φ overlying a paleo wave-cut platform (J.W. Kim et al., 2007b). The two OSL ages from the

310 sand deposits were 119±15 ka (WALIS LUM ID #442) and 111±9 ka (WALIS LUM ID #443) (Table 3; J.W. Kim et al., 2007b). Without a PWPE we estimated RSL using Eq. (8) based on its use as a beach RSL indicator (Landform Type 1 in Table 1). For that calculation, we arrive at a RSL estimate of 28.2±1.7 m and 32.2±1.7 m (Table 3; WALIS RSL ID #4016, 4017).

4.1.4 Youngduk area

315 Subsite Youngdeok-Geumgok-ri is located 20-25 m above MSL and contains rounded cobbles, pebbles, and sand deposits overlying a paleo wave-cut platform (Figs. 2, 3; S.C. Hong, 2014). Two OSL ages from quartz sand in the overlying marine deposits were interpreted as minimum ages of >44 ka and >41 ka. They appear to exceed the upper age limit of the methodology in these sediments as the traps are saturated (e.g., Rhodes, 2011). The two IRSL ages of 124.5±25.3 ka (WALIS LUM ID #444) and 122.1±24.9 ka (WALIS LUM ID #445) were obtained from the sand deposits (Table 3; S.C. Hong, 2014).

320 Without a PWPE we estimated RSL using Eq. (8) based on its use as a beach RSL indicator (Landform Type 1 in Table 1). For that calculation, we arrive at a RSL estimate of 19.4±1.7 m and 22.1±1.7 m (Table 3; WALIS RSL ID #4018, 4019).

4.2 Marine terraces along the southern east coast

4.2.1 Pohang area

This area comprises six subsites at Pohang-Josa-ri, Pohang-Ohdo-ri, Pohang-Yonghan-1 (silica mine), Pohang-Yonghan-2,
325 Pohang-Masan-ri, and Pohang-Hajeong-ri (Fig. 2). Subsite Pohang-Josa-ri is located 22 m above MSL and contains alternating beds (~1.5 m thick) of sand and silt overlying a paleo wave-cut platform (G.Y. Lee and Park, 2019b). The single OSL age from the sand deposits was 116±8 ka (WALIS LUM ID #446) (G.Y. Lee and Park, 2019b, 2020). Subsite Pohang-Ohdo-ri is located on a marine terrace 25.2 m above MSL and consists of well-rounded cobbles, pebbles, and sand (>3 m thick) (G.Y. Lee and Park, 2019b). The single OSL age from the sand deposits was 137±9 ka (WALIS LUM ID #447) (Table 3; G.Y. Lee
330 and Park, 2019b, 2020). Treating the deposits as beach sands overlying marine terraces without a PWPE and using Eq. (8) we arrived at RSL estimates of 20.2±1.7 m and 23.4±1.7 m for subsites Pohang-Josa-ri and Pohang-Ohdo-ri, respectively (Table 3; WALIS RSL ID #4020, 4021).

Subsite Pohang-Yonghan-1 (silica mine) is located on a marine terrace 32 m above MSL and contains alternating well-rounded pebble and sand beds (~1.2 m thick) (J.W. Kim et al., 2005a). A single OSL age of 123±9 ka (WALIS LUM ID #448)
335 was obtained from the sand deposits (J.W. Kim et al., 2005a). The paleo RSLs of this sample yielded 30.2±1.7 m above MSL using Eq. (8) (Table 3; WALIS RSL ID #4022).

Subsite Pohang-Yonghan-2 is located on top of a marine terrace 35 m above MSL and contains alternating paleo-beach beds (~0.5 m thick) of well-rounded pebble and sand overlain by aeolian sand beds (~8 m thick) (Fig. 4; J.H. Choi et al., 2009). The two ages from the paleo-beach sand sediments were 114±7 ka (WALIS LUM ID #449) and 127±12 ka (WALIS LUM ID #450)
340 (Table 3; J.H. Choi et al., 2009). Using Eq. (8), the paleo RSLs of these samples without a PWPE yielded 33.2±1.7 m above MSL (Table 3; WALIS RSL ID #4024). The overlying aeolian sand beds returned younger OSL ages of 104±6 ka, 108±6 ka, 92±6 ka, and 64±6 ka (not included in WALIS) in ascending stratigraphic order (Fig. 4; J.H. Choi et al., 2009). The elevation of the LIG shoreline angle is 35 m above MSL (Fig. 4; J.H. Choi et al., 2009), which, using Eq. (7), results in a LIG RSL of 33.2±1.7 m above MSL (WALIS RSL ID #4024) (Table 2).

345 Subsite Pohang-Masan-ri is located 23 m above MSL and contains paleo-beach sand beds (~0.24 m thick) and overlying aeolian sand beds (~5 m thick) above a paleo wave-cut platform (J.W. Kim et al., 2005b). The significance of the terraces in this region is also discussed by Thompson and Creveling (2021) who focus more on the MIS 5c and MIS 5a ages from this site and adjacent areas. The four ages from the paleo-beach sand sediments were 119±8 ka (WALIS LUM ID #451), 111±5 ka (WALIS LUM ID #452), 116±7 ka (WALIS LUM ID #453), and 107±8 ka (WALIS LUM ID #454) (Table 3; J.W. Kim et al.,
350 2005b). Using Eq. (8), the paleo RSLs of these samples without a PWPE yielded 21.2±1.7 m above MSL (Table 3; WALIS RSL ID #4025). A total of 158 sediment samples were also collected almost continuously from approximately 3.8 m of the

Masanri (MS) outcrop section for a paleomagnetic study (Shim, 2006). Remanent magnetic moment, alternating field demagnetization, anhysteric/isothermal remanent magnetization, and magnetic susceptibility of each sample were measured to isolate characteristic remanent magnetization (Shim, 2006). The global Blake Excursion Event was discovered in the MS

355 section on the Masan-ri marine terrace in the northern Pohang area (Fig. 2). The elevation of this outcrop section is 22 m above MSL. Considering the Blake Event (111.8 to 117.1 ka), the paleomagnetic age of the paleo-beach sediments overlying the marine terrace suggests an absolute age of 117.6±2.7 ka with an error range of between 114.9 and 120.2 ka (Table 3; Shim, 2006). At this site, the elevation of the paleo wave-cut platform is 22.0 m above MSL. Using Eq. (7), paleo RSL was estimated to be 21.7±3.2 m above MSL using 22 m PWPE and 25 m PSOE (Table 2).

360 Subsite Pohang-Hajeong-ri is located 35 m above MSL, and the section crops out in the footwall of the Hajeong fault. The section contains a wedge-shaped mix (98 to 20 cm thick) of rounded pebbles, sand, and angular alluvial pebbles overlying a marine terrace (S.J. Choi, 2016). The single OSL age from the sand was 128±12 ka (WALIS LUM ID #455) (Table 3; S.J. Choi, 2016), which is interpreted as a terrestrial limiting data point.

4.2.2 Gyeongju area

365 Subsite Gyeongju-Jinri is located on a marine terrace 36 m above MSL (Fig. 2) and contains thin (~ 15 cm thick) paleo-beach gravels underlying fine-grained sand beds (~0.5 m thick) (J.W. Kim et al., 2007a). The two OSL ages from the sand deposits were 116±6 ka (WALIS LUM ID #456) and 126±10 ka (WALIS LUM ID #457) (Table 3; J.W. Kim et al., 2007a). Using Eq. (8), the paleo RSLs of these samples without a PWPE yielded 32.3±2.6 m above MSL (Table 3; WALIS RSL ID #4027). In this area, a land seismic survey was conducted to identify the elevation of the buried paleo wave-cut platform and shoreline angle.

370 Based on seismic velocities of 600 m/s for the overlying deposits and 2100 m/s for the wave-cut platform, the elevation of the paleo wave-cut platform ranges from 27 to 29 m above MSL with a slope of 1.5° (Fig. 5; J.W. Kim et al., 2007a). Using a shoreline angle elevation of 29 m from the seismic survey, RSL is estimated to be 25.0±2.5 m above MSL (Table 2).

4.2.3 Ulsan area

Subsite Ulsan-Jeongja-ri is located 19~28 m above MSL and contains a lower unit of fluvial beds (~2 m thick), a middle unit

375 of fluvial/beach transitional beds (<1 m thick), and an upper unit of paleo-beach beds (~1 m thick) containing pebbles and sand overlying a paleo wave-cut platform (S.J. Choi et al., 2008). These terrace deposits are overlain by alternating alluvial beds (>2 m thick) of gravel, sand, and mud (S.J. Choi et al., 2008). The single OSL age from the sand deposits was 113±39 ka (WALIS LUM ID #459) (Table 3; S.J. Choi et al., 2008). Treating the sands as a beach deposit using Eq. (8) gives an RSL estimate of 18.8±2.6 m (Table 3; WALIS RSL ID #4028).

380 ### 4.2.4 Ulju area

Subsite Ulju-Weseong shows well-sorted sand of beach origin on a marine terrace at an elevation of 14 m above MSL (Fig. 2; J.H. Choi, 2004). The sand deposit was dated to 112±7 ka (WALIS LUM ID #458) (Table 3; J.H. Choi et al., 2003; J.H. Choi,

2004). Using Eq. (8), the paleo RSLs of these samples without a PWPE yielded 10.3±2.6 m above MSL (Table 3; WALIS RSL ID #4029). Thompson and Creveling (2021) discuss the sea-level significance of this site and adjacent areas in their summary of MIS5c and MIS5a sea levels.

4.2.5 Sacheon area

The Sacheon area is located in the south-facing Korean Peninsula straddling the eastern and western coasts (Fig. 2). Subsite Sacheon-Daepo-dong lies at ~6 m above MSL and unlike the LIG shorelines of the eastern Korean Peninsula is not marked by a distinctive marine terrace geomorphology (J.Y. Shin and Hong, 2018). The paleo-shoreline deposits (2-3.5 m thick) are characterized by clast-supported well-rounded cobble and pebble deposits with little to no matrix. Their sedimentary characteristics are similar to the sandy gravel bars of the modern upper tidal flats in the region (J.Y. Shin and Hong, 2018). Two OSL rock-surface ages obtained from cobbles were 111.2±16.0 ka (WALIS LUM ID #460) and 102.5±14.7 ka (WALIS LUM ID #461) (Table 3; J.Y. Shin and Hong, 2018). Based on Eq. (9), we arrive at a RSL estimate of 6.0±0.8 m (Table 3; WALIS RSL ID #4030).

4.3 Onshore paleo-beach and terrestrial deposits of the west coast

4.3.1 Wando area

Subsite Wando-Sinji has two localities at approximately 3 m and 6 m above MSL (G.R. Lee and Park, 2018; W.J. Shin et al., 2019). At the 3 m site, a 0.3 to 1 m thick shell-bearing sand with well-rounded pebbles and cobbles is interpreted to represent a paleo-beach deposit. Its sedimentary facies is similar to the modern sandy gravel tidal-beach or intertidal deposits of the modern upper tidal flats of the region (W.J. Shin et al., 2019). The five OSL ages acquired from the deposits at 2.55, 2.80, 3.50, 4.25, and 4.50 m above MSL were 157.4±18.9, 127.5±8.5, 115.9±9.7, 23.2±1.2, and 6.2±0.4 ka, respectively (W.J. Shin et al., 2019). Only the two MIS 5e ages of 127.5±8.5 ka (WALIS LUM ID #462) and 115.9±9.7 ka (WALIS LUM ID #463) were included in the WALIS database (Table 3; W.J. Shin et al., 2019). Based on Eq. (9), we arrive at a RSL estimate of 2.5±0.9 m and 3.2±0.9 m (Table 3; WALIS RSL ID #4031).

At the 6 m locality, 4 m of sand and well-rounded cobbles and boulders are thought to represent a paleo-beach deposit (G.R. Lee and Park, 2018). The single age from the sand deposits was 108±18 ka (WALIS LUM ID #464) (Table 3; G.R. Lee and Park, 2018, 2019a). Based on Eq. (9), we arrive at a RSL estimate of 5.8±0.9 m (Table 3; WALIS RSL ID #4032).

4.3.2 Haenam area

Subsite Haenam-Ijin-ri is located 4-8 m above MSL and is comprised of sandy and clayey silt beds with granules and pebbles (D.Y. Yang et al., 2016). The gravel is a mixture of rounded to sub-angular clasts. These deposits were originally interpreted as marine sediments within a marine terrace, based on chemical analysis of the clay minerals (D.Y. Yang et al., 2016). However, no distinctive sedimentological and geomorphologic characteristics of the deposit suggest a marine origin. On the contrary,

the poorly sorted sandy/clayey silt deposits with dispersed gravels look like overwash deposits in a backshore or alluvial setting behind the shoreline (e.g., J.Y. Lee et al., 2013; K.H. Choi et al., 2014). Four OSL ages acquired from the deposits at 4.95,
415   5.41, 6.49, and 7.51 m above MSL in the outcrop were dated as 152±11 (not included in WALIS), 128±9, 128±10, and 121±10 ka, respectively (D.Y. Yang et al., 2016). The three MIS 5e ages from the fine-grained silt sediments of 128±9 ka (WALIS LUM ID #467), 128±10 ka (WALIS LUM ID #466), and 121±10 ka (WALIS LUM ID #465) (Table 3; D.Y. Yang et al., 2016) are included in the WALIS database and interpreted as terrestrial limiting records of 4.3±1.3, 5.3±1.3, and 6.4±1.3 m, respectively (Table 3).

4.3.3 Buan area

420

The Buan area on the west coast of the Korean Peninsula (Fig. 7) has two localities, Daehang-ri and Mapo-ri, located 11 m and 9 m above MSL, respectively (G.R. Lee and Park, 2018). At the two localities, the outcrop exposes a mixture of silt, sand, and well-rounded pebbles and cobbles, approximately 2 m thick (G.R. Lee and Park, 2018). These deposits were originally interpreted as alluvial or marine sediments (G.R. Lee and Park, 2018) with little distinctive sedimentological or
425   geomorphologic evidence for a marine origin. The two OSL ages from the sandy sediments were 112±24 ka (WALIS LUM ID #468) and 130±20 ka (WALIS LUM ID #469) (Table 3; G.R. Lee and Park, 2018, 2019a), which are interpreted as terrestrial limiting records.

4.4 Paleo-intertidal and nearshore deposits of the west coast

4.4.1 Seocheon area

430   Core DSR-C03 was collected onshore of a modern high-tide beach near Seocheon on the west coast of the Korean Peninsula (Fig. 7; Chang et al., 2017). MIS 5e deposits occur lower than about 1.5 m below MSL (Fig. 9). These occurrences of LIG deposits at approximately -1.5 m in elevation are the shallowest LIG deposits found on the west coast of the Korean Peninsula. Four depositional units labeled as Units A, B1, B2, and C, in ascending stratigraphic order, were identified based on sediment texture and structures (Figs. 9, 10).

435   #### 4.4.1.1 Unit A

The lowermost Unit A is mud-rich with sandy beds showing an overall coarsening-upward trend and attains a thickness of up to 12.5 m in core DSR-C03 (Fig. 9). This unit is comprised of lower muddy beds and upper more sandy beds (Fig. 9), both of which contain tidal couplets of mud and sand (Fig. 10D, E). The lower muddy beds are characterized by intense bioturbation, no shell or rare shell fragments, and lenticular to wavy tidal bedding, while the upper more sandy beds show moderate
440   bioturbation, few shell fragments, and flaser to wavy and lenticular tidal bedding. Considering the presence of mud-sand tidal bedding and muddy nature of the sediments with no shell or rare shell fragments, the lower muddy beds are interpreted as being deposited in upper mud-flat or salt-marsh environments (e.g., Klein, 1985; Dalrymple et al., 1992; Dalrymple, 2010).

cancel

The upper moderately bioturbated more sandy beds are suggestive of being deposited in an intertidal mixed-flat environment. The uppermost part of Unit A resembles the pre-Holocene semi-consolidated oxidized beds commonly occurring on top of

445   tidal-flat sequences throughout the west coast of Korea (e.g., Y.H. Kim et al., 1999; Lim et al. 2004; H.H. Yoon et al., 2021). The two OSL ages of 116±10 ka and 108±8 ka suggest that the tidal deposit formed during the MIS 5 period (Table 3; Fig. 9; e.g., Chang et al. 2014; Baek et al. 2017; H.H. Yoon et al., 2021).
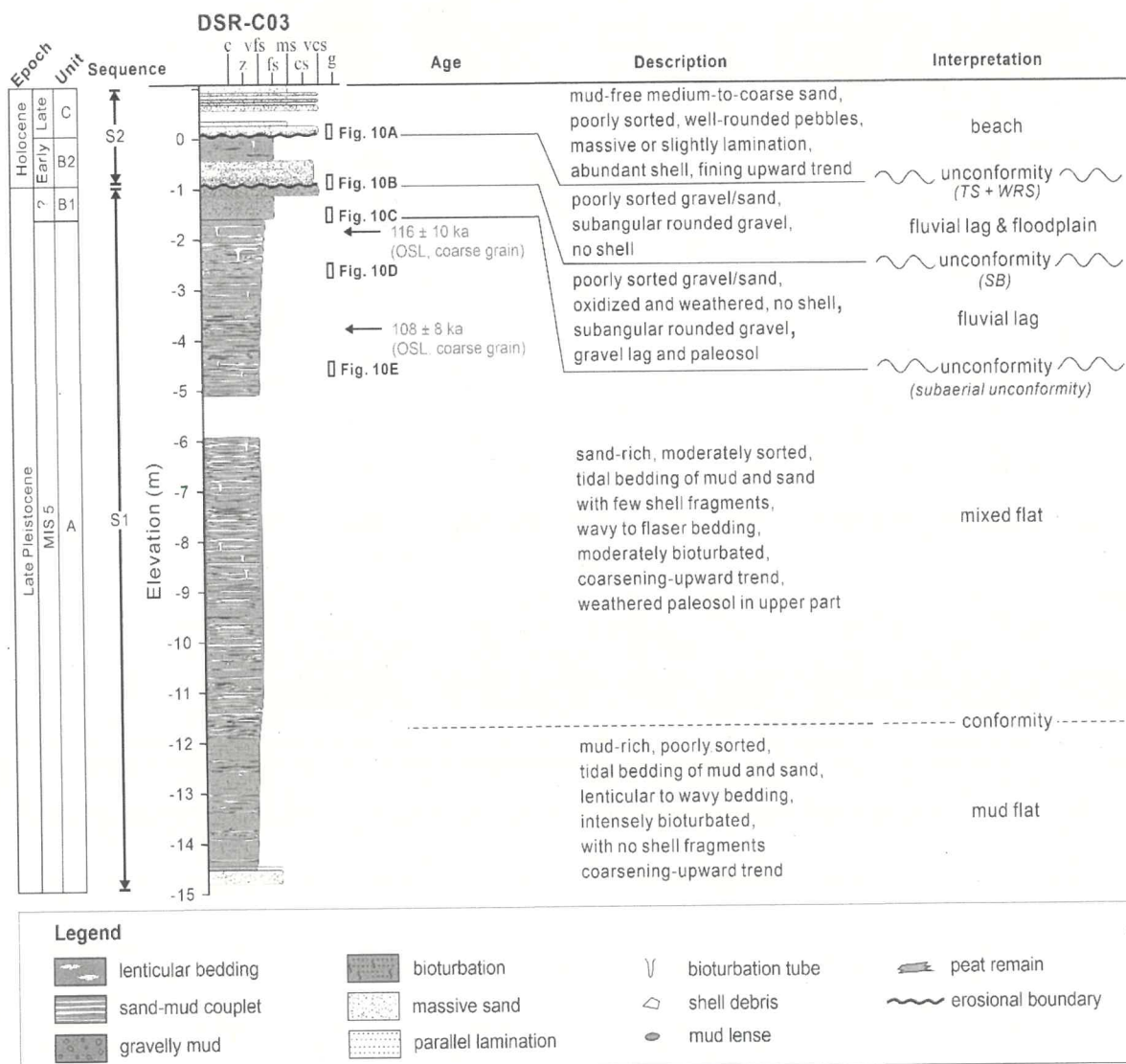
450   **Figure 9: Schematic columnar section of core DSR-C03 including lithology and OSL ages (cf. Chang et al., 2017). Age data are referred to in Table 3. For the location of the core, see Fig. 7. TS: Transgressive Surface, WRS: Wave Ravinement Surface, SB: Sequence Boundary**
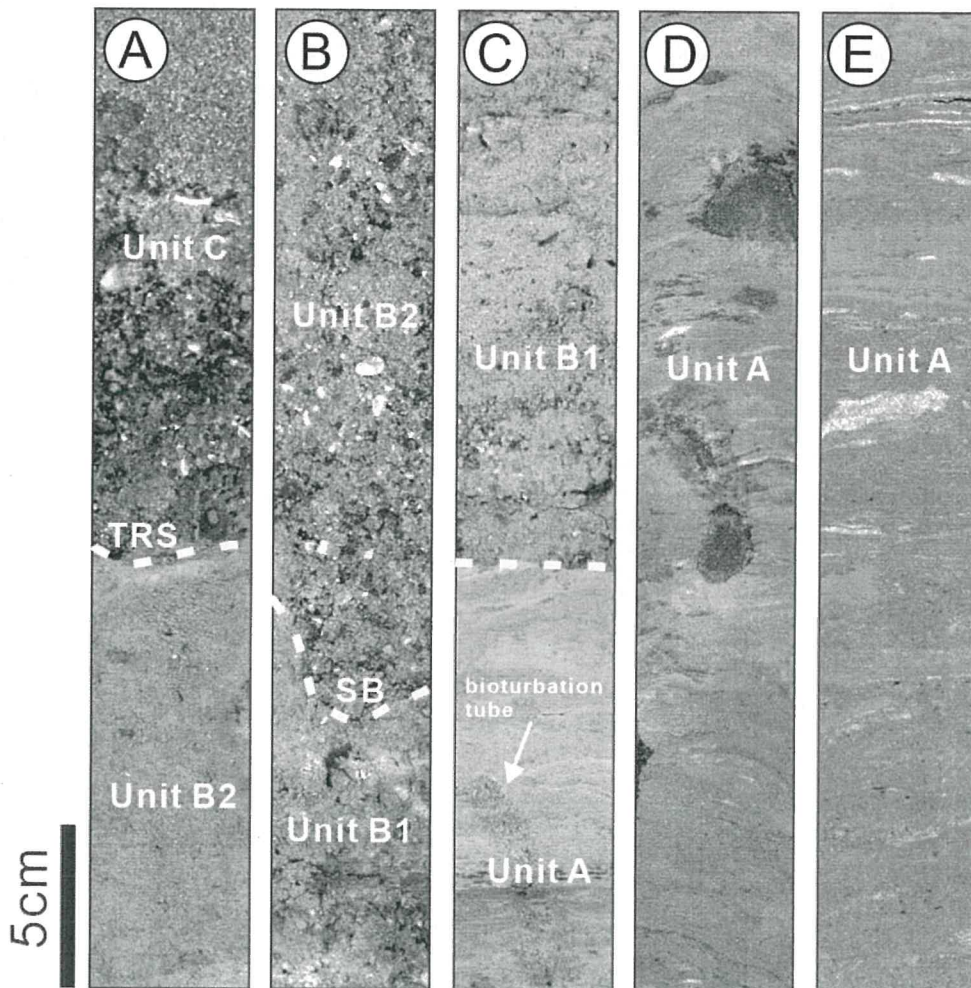
Figure 10: Selected photographs of core sediments in core DSR-C03 in Fig. 9. (a) Massive mud-free sand beds with laminated sand,
455 **pebble, shell-rich layers (Unit C). (b) Muddy coarse-grained sediments with relatively less oxidized poorly sorted gravel and sand**
(Unit B2). (c) Completely oxidized poorly sorted gravel and sand without muddy sediments (Unit B1). (d, e) Moderately bioturbated,
laminated, sandy mud and muddy sand with moderate amounts of flaser, wavy to lenticular bedding and rhythmic lamination (Unit
A). The oxidized upper part of Unit A is reddish while the lower part has a gray color. TRS: Transgressive Ravinement Surface, SB:
Sequence Boundary

460

Two OSL ages were obtained from Unit A in core DSR-C03. The one MIS 5e OSL age obtained from a coarse quartz sand

bed was 116±10 ka (WALIS LUM ID #470) at -3.01 m below MSL. Another MIS 5e/5c OSL age of 108±8 ka (WALIS LUM

ID #471) was obtained at a core depth of -4.95 m below MSL (Table 3; Chang et al., 2017). The shallow occurrence of LIG

deposits in Unit A represents the highest among marine limiting records of LIG RSL.

465 OSL-dated clastic tidal-flat deposits were used as paleo RSL markers, identified based on sediment texture and sedimentary

structures, and interpreted as tidal environments (e.g., Mauz and Bungenstock, 2007). Although some interpretations are of

salt-marsh deposits or intertidal mixed-flat deposits, no microfaunal work has been conducted on the deposits to confirm their marsh and mixed-flat interpretations and thus tightly constrained relationship with paleo-sea levels as is normally done in other salt-marsh or intertidal based RSL studies (e.g., Shennan et al., 2015). Thus the tidal-flat data points are treated as marine
470   limiting records because their relationship to past tidal-datums is not constrained by biological indicators.

4.4.1.2 Unit B

Unit B is approximately 2 m thick and is separated from the underlying Unit A by a distinct erosional boundary (Figs. 9, 10C). This unit can be further subdivided into two subunits: the lower unit B1 consists of completely oxidized gravel and sand devoid of muddy sediments and the upper unit B2 contains muddy sediments with less oxidized gravel and sand sediments compared
475   to unit B1. The sediments are composed of poorly sorted gravel and coarse sand (Fig. 10B, C). These units contain neither shells, foraminifers nor any other marine indicators. Muddy deposits of Unit B2 are commonly associated with coarser sand layers and contain wood fragments, fine peat, and rootlets. The erosional unconformities at the base of Units B1 and B2 and the presence of oxidized sediments point to an extended period of subaerial exposure. The contact is interpreted as a sequence boundary (Figs. 9, 10B). The coarse-grained sediments without a muddy matrix probably originated from gravel bars or
480   channel lag deposits in a fluvial environment (e.g., K. Choi and Kim 2006; Chang et al. 2014; Baek et al. 2017).

4.4.1.3 Unit C

Unit C is characterized by an upper massive sand bed and a lower crudely stratified sand bed showing a fining-upward trend (Fig. 9). The sand beds are mud-free and contain shell-rich beds (Fig. 10A). The upper sand beds are a few decimeters thick, structureless, and comprised of very poorly sorted medium to coarse yellowish sand. The lower crudely stratified sand beds
485   contain granules and pebbles (Fig. 10A). These characteristics suggest a swash deposit in the beach face. Unit C rests on a sharp erosional boundary separating it from the underlying sand/mud deposits of Unit B2 (Figs. 9, 10A). The erosional boundary is interpreted as a transgressive ravinement surface, formed by landward shoreface retreat and wave action in a shoreline during transgression and thus these deposits likely post-date the last glacial maximum (Fig. 9).

OSL?

4.4.2 Younggwang area

490   Two cores were obtained on a modern tidal flat at Baeksu and Baeksu-Duuri near Younggwang (Fig. 7; Chang et al., 2014; Baek et al., 2017). Core 11YG-C4 at Baeksu has approximately 18 m of LIG deposits between -38 and -20 m below MSL (Fig. 11). The LIG deposit is characterized by tidal rhythmites, sand-mud couplets, and a lower stiff tidal mud with fine peats, rootlets, and wood fragments (Chang et al., 2014). The characteristics of LIG deposit are indicative of deposition within a tidal mud-flat and salt-marsh environment (Chang et al., 2014). The twelve LIG ages from the fine quartz were 110.0±6.6 ka
495   (WALIS LUM ID #472) at -20.8 m in elevation, 133.9±7.6 ka (WALIS LUM ID #473) at -22.1, 124.0±7.8 ka (WALIS LUM ID #474) at -23.9 m, 138.8±7.8 ka (WALIS LUM ID #475) at -25.2 m, 128.7±7.9 ka (WALIS LUM ID #476) at -26.8 m, 124.7±7.6 ka (WALIS LUM ID #477) at -28.3 m, 118.8±7.0 ka (WALIS LUM ID #478) at -29.8 m, 112.2±6.8 ka (WALIS

LUM ID #479) at -31.3 m, 113.4±7.1 ka (WALIS LUM ID #480) at -32.8 m, 118.2±7.4 ka (WALIS LUM ID #481) at -34.3 m, 112.6±6.9 ka (WALIS LUM ID #482) at -35.8 m, and 113.1±7.3 ka (WALIS LUM ID #483) at -37.3 m in elevation (Table 3; Chang et al. 2014). These occurrences suggest marine limiting records of LIG RSL.

In core 11YG-C01 from Baeksu-Duuri, LIG deposits occur between -31 and -19 m below MSL (Fig. 11). The LIG deposit attains a thickness up to approximately 12 m in the core and is characterized by tidal rhythmites, sand-mud couplets, a massive sand bed, and a fully bioturbated bed representative of tidal mud-flat and salt-marsh environments (Baek et al., 2017). It also contains shell beds, a lower stiff silt, mottled mud, partly deformed mud, fine peats, and wood fragments (Baek et al., 2017). The three LIG ages from the fine quartz were 107.7±6.7 ka (WALIS LUM ID #484) at -15.5 m in elevation, 122.1±7.2 ka (WALIS LUM ID #485) at -26.0, and 126.2±8.1 ka (WALIS LUM ID #486) at -27.3 m in elevation (Table 3; Baek et al., 2017), suggesting marine limiting records of LIG RSL.

4.4.3 Gochang area

Core 15DH-C03 in the Gochang area was obtained from the modern nearshore environment and contains LIG deposits between -32 and -39 m below MSL (Figs. 7, 8; H.H. Yoon et al., 2021). The LIG deposit attains a thickness of up to approximately 7 m in the core, which is characterized by muddy beds containing no shell or rare shell fragments (Fig. 11; H.H. Yoon et al., 2021). Sediments in the lower part of the core mainly consist of laminated mud beds with some mud-sand couplets or lenticular bedding. The sediments contain a few bioturbated beds. Sediments in the upper part of the core are largely mottled, intensely bioturbated, and composed dominantly of silty mud. The sediments contain some dark-gray organic-rich beds with wood fragments. Based on the presence of mud-sand couplets and lenticular bedding, the lower laminated mud beds are interpreted as being deposited in an upper mudflat environment (H.H. Yoon et al., 2021). The upper bioturbated mud with some organic material suggests deposition within a tidal salt-marsh environment (H.H. Yoon et al., 2021). The presence of tidal mud-sand couplets and ages between MIS 5e and 5d suggests that the tidal deposit formed during or shortly after the LIG period (e.g., Chang et al. 2014; Baek et al. 2017).

The three MIS 5 ages from the fine quartz were 107.5±7.6 ka (WALIS LUM ID #487) at -35.2 m below MSL, 107.6±7.3 ka (WALIS LUM ID #488) at -37.4 m below MSL, and 113.3±7.2 ka (WALIS LUM ID #489) at -38.2 m below MSL (Table 3; H.H. Yoon et al., 2021), suggesting marine limiting records of LIG RSL.

4.4.4 Jindo area

Core H-C11 was obtained from the region offshore and south of Jindo (Fig. 7). A LIG age was obtained from sediments at an elevation of -48.5 m (S.H. Hong et al., 2019). This massive sandy shell bed was interpreted as a shelf deposit, based on the presence of faint swaley cross-bedding and abundant oyster fragments (Fig. 11; S.H. Hong et al., 2019). The single LIG age from fine quartz sand was 124.4±10.0 ka (WALIS LUM ID #490) at an elevation of -48.5 m (Table 3; S.H. Hong et al., 2019). This deposit provides a marine limiting record of LIG RSL.
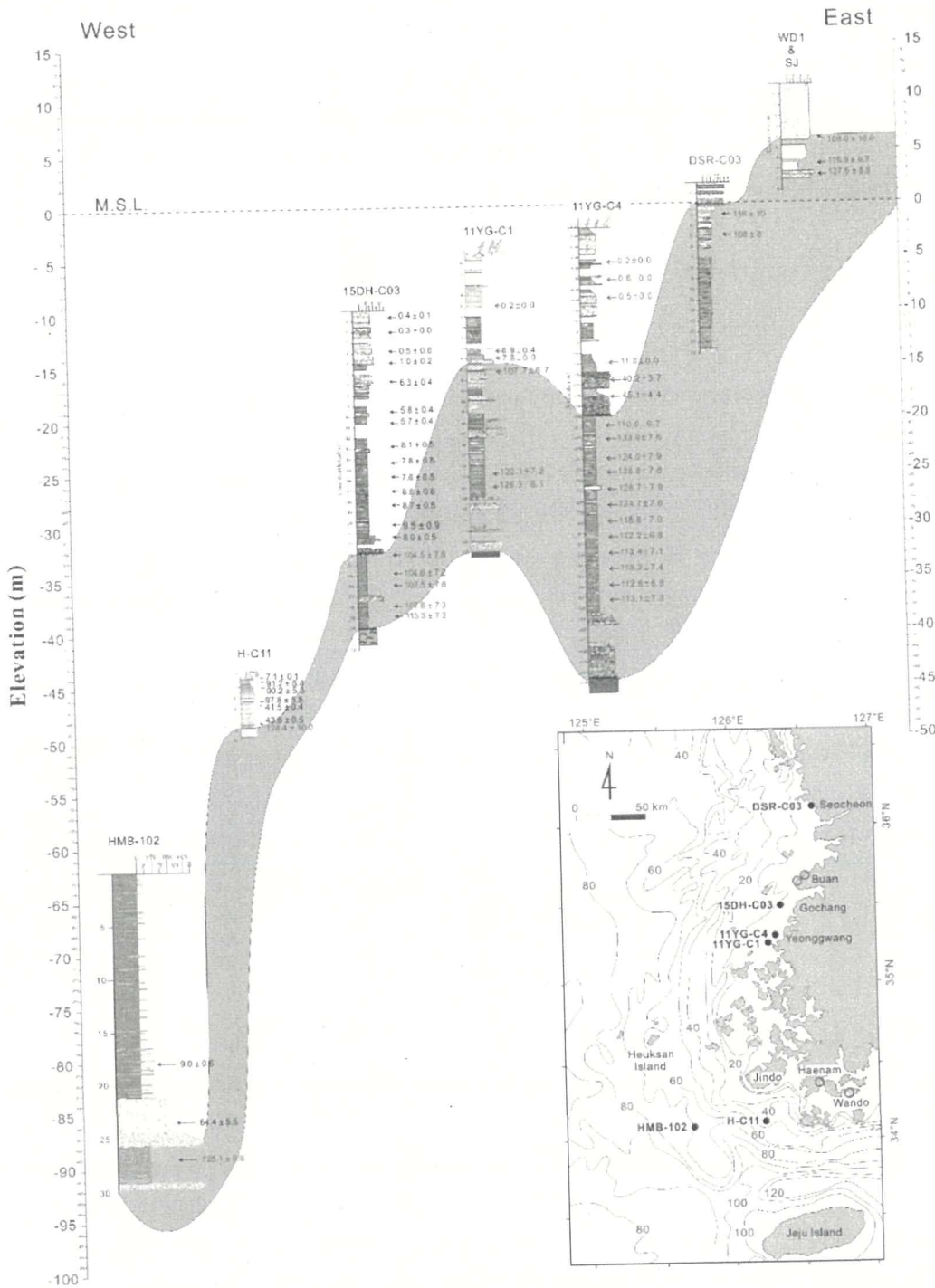
530

Figure 11: Arrangement of onshore sections (WD1 and SJ) and tidal-to-nearshore core sections (DSR-C03 to HMB-102) in the west coast of Korea according to the elevation of the remnant LIG deposits. For location, see Fig. 7.

4.4.5 Heuksan Mud Belt area

535   Core HMB-102 of the Heuksan Mud Belt was obtained from the modern offshore environment (Fig. 7). One LIG age in the core was obtained at -84 m from a tidal deposit of laminated silt and clay and mottled mud (Fig. 11; Chang and Ha, 2015). The single LIG age from fine quartz sand was 125.1±9.9 ka (WALIS LUM ID #491) at an elevation of -84 m (Table 3; J. C. Kim et al., 2019). This deposit represents a marine limiting record of LIG RSL.

5. Related sea-level topics

5.1 Uplift

540   The seismic stratigraphy and geology of the Gangneung and Donghae areas of the east coast of South Korea were summarized by Kwon et al. (2009) and Ryang et al. (2014). Intense compressional deformation during the early Pliocene, accompanied by the formation of reverse faults, strike-slip faults, and anticlinal folds, occurred mainly along the western margin of the submerged South Korea Plateau of the East Sea (Fig. 12; Ryang et al., 2007; Kwon et al., 2009). This deformation resulted in partial uplift and erosion of Late Pliocene and Early Quaternary deposits (Fig. 13). The lower boundaries of the post-Miocene
545   stratigraphic units represent a progressive onlap termination against the apices of anticlinal folding (Fig. 13; Kwon, 2005; Kwon et al., 2009).

The southern region of the east coast may have also experienced considerable vertical displacement and deformation reflecting tectonic uplift during the Late Pleistocene along regional faults such as the Hupo, Yangsan, Ulsan faults (J.H. Choi et al., 2003, 2009; S.J. Choi et al., 2008). All of the distorted uplifts are interpreted to be the result of backarc closing under a
550   compressional regime since the early Pliocene (5 Ma) (S.H. Yoon and Chough, 1995; Chough et al., 2000). Although not all of the cross-coast faults along the east coast have been documented, local vertical movement and deformation probably caused raise marine terraces to uplift at different rates (Figs. 14, 15). This suggests contaminated elevations as a result of distorted tectonic uplift (e.g., J.H. Choi et al., 2003, 2009; S.J. Choi et al., 2008, 2016).

5.2 Subsidence

555   The currently-dated LIG sites along the west coast of Korea are all subject to possible subsidence rather than tectonic uplift. LIG deposits are found at lower elevations with greater water depth but these likely reflect deposition in progressively deeper waters (Figs 1, 11). LIG deposits appear to be better preserved basinward (Fig. 15). This preservation may be a result of erosion of the higher LIG deposits during subsequent sea-level falls (e.g., MIS 5d – MIS 2). Preservation of the deeper LIG deposits may have also been aided by their tectonic setting with increasing subsidence basinward. However, constraining the magnitude
560   of Quaternary subsidence independent of the LIG elevation has yet to be attempted. Regional tectonic studies independent of the LIG shoreline elevation are needed to determine subsidence rates and correct LIG sea levels from its influence.

Earth System Discussions

Science
Data
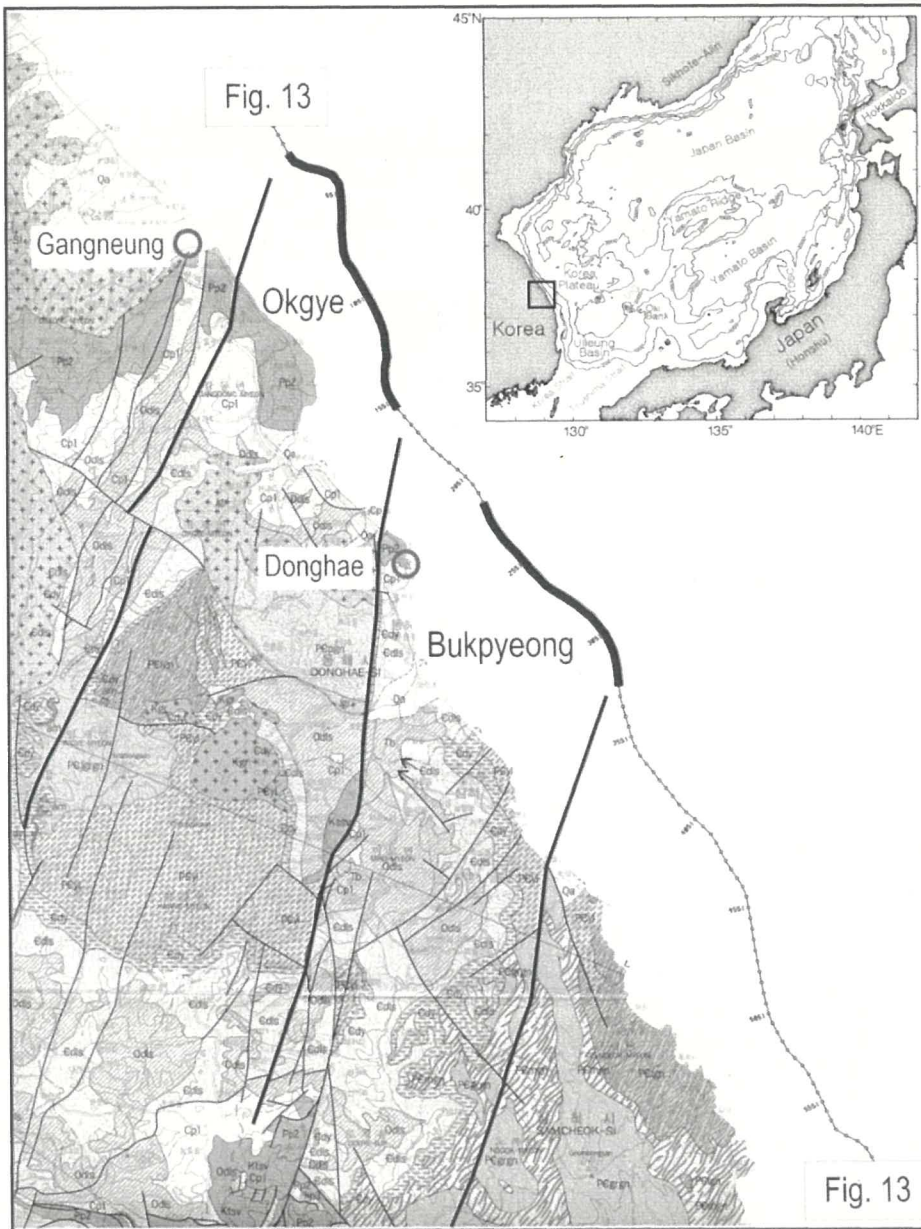
Figure 12: Geological map (1:250,000) and seismic track line around the Gangneung and Donghae areas (modified after J.C. Kim
et al., 2005; Ryang et al., 2007, 2014). The multichannel seismic profile with interpretation is shown in Fig. 12. Red circles indicate
the sampling areas for LIG ages in Fig. 2. Solid lines indicate major faults of strike-slip or thrust origin. Two thick parts of the track
line represent the interval of thick sedimentary bodies in the seismic profile of Fig. 12. Inset shows this figure area (solid rectangle)
and adjacent land and sea (Chough et al., 2000). Legend codes of the geologic map (J.C. Kim et al., 2005): Qa, Quaternary Alluvium;
Tb, Tertiary Bukpyeong Group; Kgr, Cretaceous granite; Kssv, Ktsv, Cretaceous Kyeongsang Supergroup; Jgr, Jurassic granite;
Pp2, Permian Middle Pyeongan Group; Cp1, Carboniferous Lower Pyeongan Group; Odls, Ordovician Upper Great Limestone
Group; Ꞓdls, Cambrian Lower Great Limestone Group; Ꞓdy, Cambrian Yangduk Group; Pꞓjgrgn, Pꞓgrgn, Pꞓlgn, Pꞓmgn, Pꞓyl,
Precambrian Metamorphic Complex.
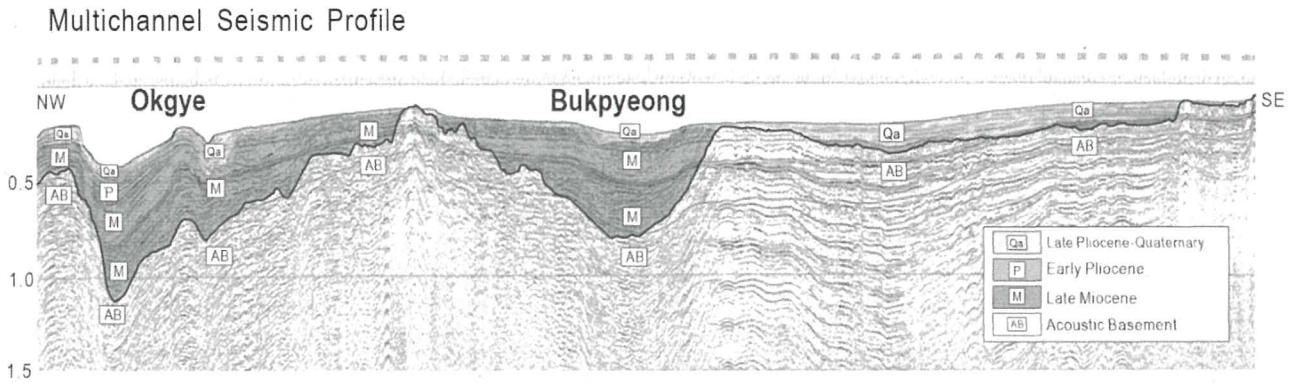
Figure 13: Parallel seismic section to the coastline and its stratigraphic interpretation (modified after Kwon, 2005; Ryang et al., 2007, 2014). For the seismic track line, see Fig. 12.
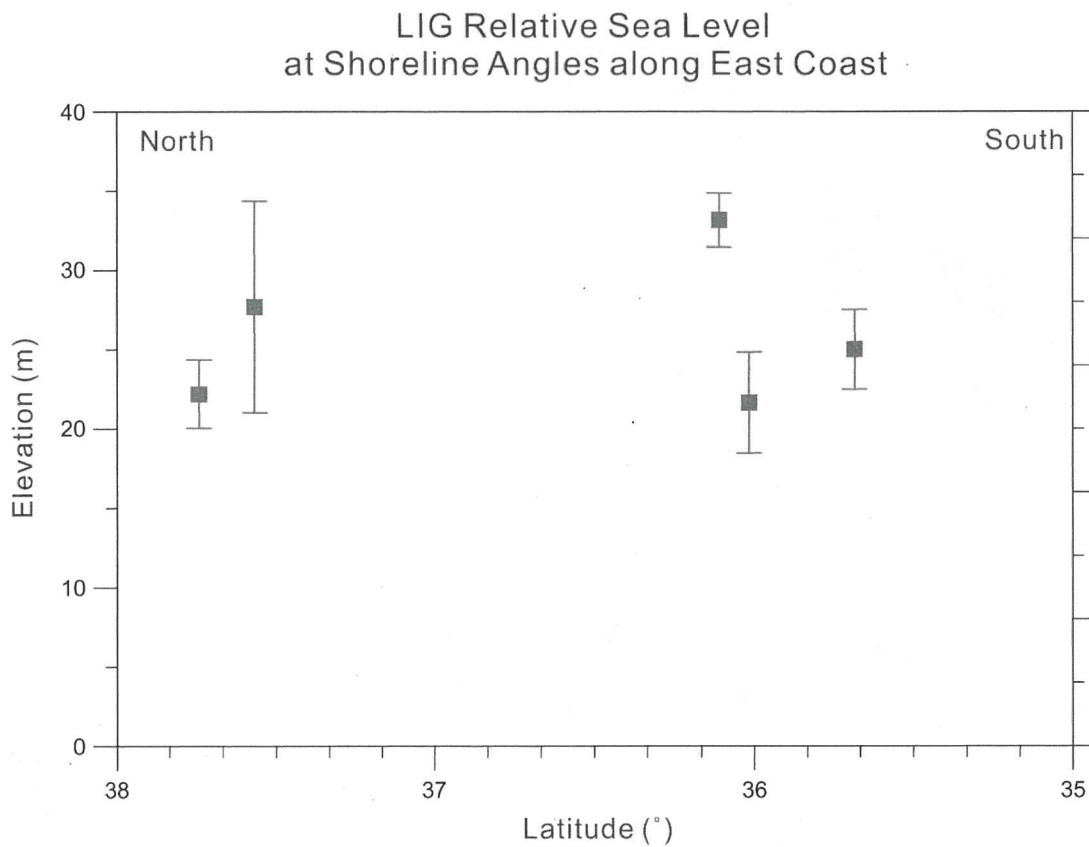
Figure 14: LIG relative sea level of the shoreline angles according to latitude along the east coast of Korea. For detailed data, refer to Table 2.
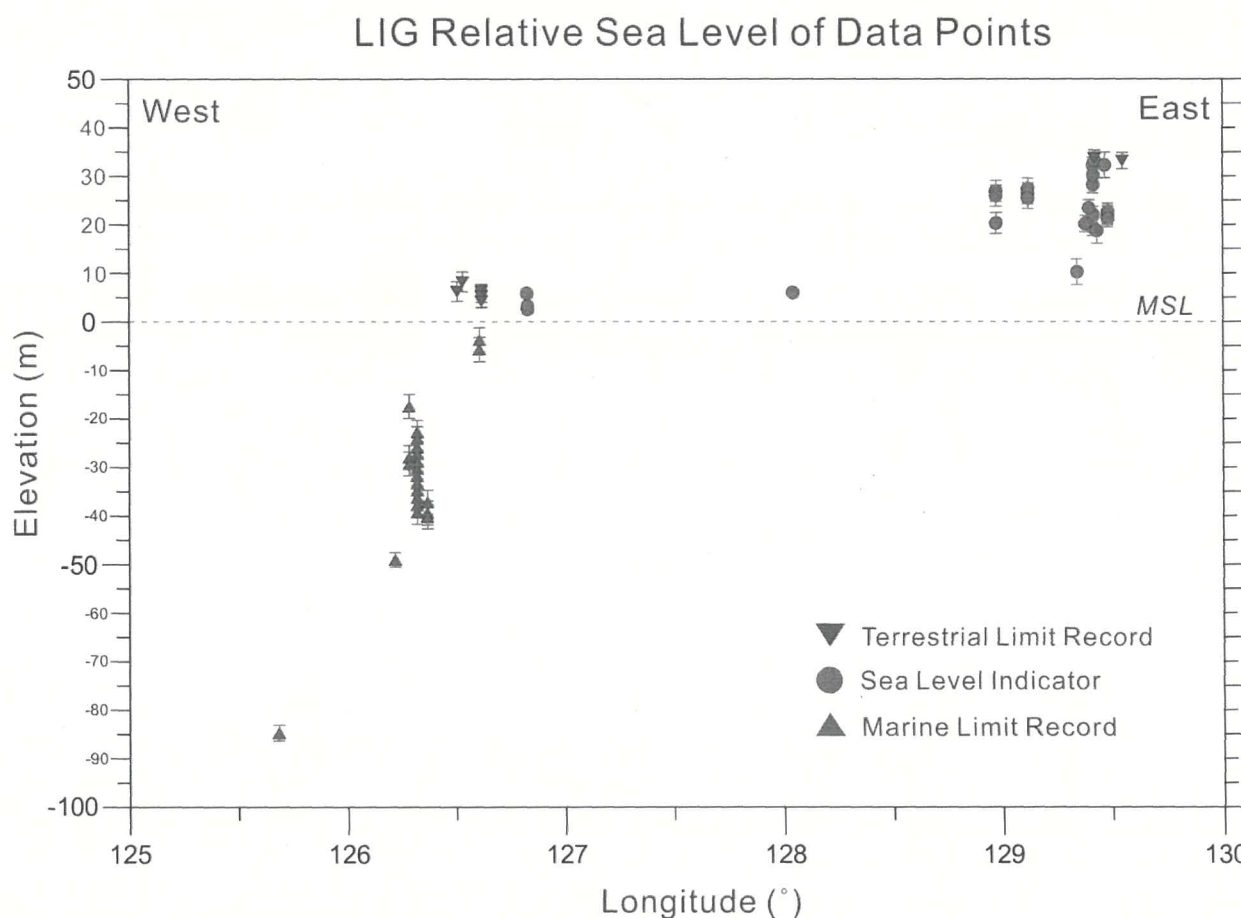
580

Figure 15. LIG relative sea level of data points according to longitude across the Korean Peninsula. For detailed data, refer to Table 3.

5.3 LIG sea-level fluctuations

Most ages of the LIG features in the Korean Peninsula were dated by OSL. The error range of the OSL method is too large for
585 the confident identification of fine-scale fluctuations in LIG sea levels. Relatively few occurrences of LIG deposits also limit
tests for LIG sea-level fluctuations along the Korean Peninsula.

5.4 Earlier highstands

Four IRSL ages ranging from 185 to 221 ka were obtained from paleo-beach deposits on marine terraces of earlier highstands
at 59 to 63 m above MSL in the Gangneung area of the east Korean coast (Fig. 2; S.C. Hong, 2014). In this area, three ages
590 between 211 and 253 ka were also dated by cosmogenic [10]Be dating of paleo-beach deposits on marine terraces at 61 to 66 m

above MSL (S.Y. Lee et al., 2015). More work is needed to better document earlier sea-level highstands on the Korean Peninsula.

5.5 Holocene sea-level indicators

Representative Holocene sea-level curves are well constrained based on intertidal features and other sea-level indicators along the west coast of the Korean Peninsula (Bloom and Park, 1985; Y.H. Kim et al., 1999; Chang and Choi, 2001; Chough et al., 2004; E. Lee and Chang, 2015). However, the curves are limited by the absence of preserved tidal deposits as well as sparse ages on tidal-flat sea-level indicators from 6500 to 3000 yrs ago, dissimilar to those of the Yangtze delta plain in China (Chough et al., 2004; S.J. Choi, 2018; H.H. Yoon et al., 2021). K.H. Choi (2009) suggested the possibility of a sea-level highstand around 6000 yrs based on OSL-dated onland sand dune deposition, but he also noted the absence of age data covering the period between 5000 and 3500 yrs ago in his study. Another suggestion is the possibility of a higher-than-present mid-Holocene highstand based on palynological data on land (Hwang and Yoon, 2011; Song et al., 2018), but these deposits lack a proper sedimentological description and stratigraphic framework. Further work remains to be done in reconstructing mid-Holocene sea levels along the Korean Peninsula.

5.6 Uncertainty and data quality

As all the summarized age data are based on OSL, except for a single paleomagnetic age, the ages of the LIG shoreline features in the Korean Peninsula are only accurate and precise enough to establish a MIS 5 age, not necessarily which interstadial the features were deposited during. The amount of age uncertainty depends on the mineral type dated, either quartz or K-feldspar. The average error of the 42 OSL measurements using quartz minerals is 9.7 ka, and that of the 10 OSL measurements on K-feldspar minerals is 20.7 ka. The large age uncertainty in dating of K-feldspar minerals is more than double that of dating quartz. This range of 9.7 to 20.7 ka is thought to be far too large to determine exactly within MIS 5 the deposits formed. However, based on their stratigraphic occurrences as the highest deposits from the region, we interpret most of the OSL-dated deposits as MIS 5e in age. Although the basement massif in the west coast of Korea has been assumed to be stable or undergoing minor subsidence during the Quaternary (Chough et al., 2010), the uncertainty of LIG sea levels is probably not free of additional error from possible subsidence or uplift around the Korean Peninsula.

6 Concluding remarks

The LIG shoreline is well developed as a marine terrace along the east coast of the Korean Peninsula and MIS 5 deposits are prevalent within the onshore and nearshore west coast. The east coast contains prevalent beach deposits on many marine terraces along the peninsula. The east coast LIG deposits suggest RSLs between +9 and +32 m (Table 3; Fig. 15). However, the uplifted terraces are likely distorted by faulting under a compressional regime as a result of backarc closing of the East Sea (Table 2; Fig. 14). As a result, the distorted tectonic uplift likely contaminates the elevation of the east coast LIG shorelines.

On the contrary, LIG sea levels appear to be well constrained to between +2 and +5 m by marine limiting records, sea-level indicators, and terrestrial limiting records along the west coast of the Korean Peninsula (Table 3; Fig. 15); the most stable side of the Peninsula, although minor subsidence of the western coast cannot be ruled out. Further work is needed to establish credible sea-level indicators within the onshore portions of the west coast of the Korean Peninsula.

625 **7 Data availability**

The Korean Peninsula Last Interglacial sea-level database is available open access, and updated as necessary, at the following link: https://doi.org/10.5281/zenodo.4974826. The files at this link were exported from the WALIS database interface on August 26, 2020. Description of each field in the database is contained at this link: https://doi.org/10.5281/zenodo.3961543 (Rovere et al., 2020) and is accessible and searchable here: https://walis-help.readthedocs.io/en/latest/. More information on 630 the World Atlas of Last Interglacial Shorelines can be found here: https://warmcoasts.eu/world-atlas.html.

Author contributions

WHR read the papers for the data, compiled the data, and wrote the initial manuscript. ARS coined this work and revised the manuscript and dataset. HHY wrote the section of core DSR-C03 and drew most of the modified and original figures in this paper. Further input and discussion on the data and manuscript were provided by SSC and GSK. All authors revised the final 635 text and agree with its contents.

Acknowledgments

This research was supported by research funds of Jeonbuk National University in 2020 and the National Research Foundation of Korea (NRF) grant funded by the Korean government (MSIT) (NRF-2019R1F1A1057715). The data used in this study were compiled in WALIS, a sea-level database interface developed by the ERC Starting Grant "WARMCOASTS" (ERC-StG-640 802414), in collaboration with PALSEA (PAGES / INQUA) working group. The database structure was designed by A. Rovere, D. Ryan, T. Lorscheid, A. Dutton, P. Chutcharavan, D. Brill, N. Jankowski, D. Mueller, M. Bartz, E. Gowan, and K. Cohen.

References

Baek, Y. S., Lee, S. H., and Chang, T. S.: Last interglacial to Holocene sedimentation on intertidal to subtidal flats revealed by seismic and deep-core sediment analyses, southwest coast of Korea, Quaternary International, 459, 45-54, 2017.
645 Bradley, W. C., and Griggs, G. B.: Form, genesis, and deformation of central California wave-cut platforms, Geological Society of America Bulletin, 87, 433-449, 1976.

Earth System
Science
Data

Bloom, A. L. and Park, Y. A.: Holocene sea-level history and tectonic movements, Republic of Korea, The Quaternary Research, 24, 77-84, 1985.

Chang, J. H. and Choi, J. Y.: Tidal-flat sequence controlled by Holocene sea-level rise in Gomso Bay, west coast of Korea, Estuarine, Coastal and Shelf Science, 52, 391-399, 2001.

Chang, T. S. and Ha, H. J.: The Heuksan mud belt on the tide-dominated shelf of Korea: a supply-driven depositional system? Geo-Marine Letters, 35, 447-460, 2015.

Chang, T. S., Kim, J. C., and Yi, S.: Discovery of Eemian marine deposits along the Baeksu tidal shore, southwest coast of Korea, Quaternary International, 349, 409-418, 2014.

Chang, T. S., Hong, S. H., Chun, S. S., and Choi, J. H.: Age and morphodynamics of a sandy beach fronted by a macrotidal mud flat along the west coast of Korea: a lateral headland bypass model for beach-dune formation, Geo-Marine Letters, 37, 361-371, 2017.

Choi, J. H.: Luminescence ages of quaternary marine sediments on the eastern coast of Korea and their geomorphic implications, Ph.D. thesis, Seoul National University, Republic of Korea, 137 pp., 2004.

Choi, J. H., Murray, A. S., Cheong, C. S., Hong, D. G., and Chang, H. W.: The resolution of stratigraphic inconsistency in the luminescence ages of marine terrace sediments from Korea, Quaternary Science Reviews, 22, 1201-1206, 2003.

Choi, J. H., Cheong, C. S., and Chang, H. W., 2004, Principles of quartz OSL (Optically Stimulated Luminescence) dating and its applications, Journal of the Geological Society of Korea, 40, 567-583, 2004 (in Korean with English abstract)

Choi, J. H., Kim, J. W., Murray, A. S., Hong, D. G., Chang, H. W., and Cheong, C. S.: OSL dating of marine terrace sediments on the southeastern coast of Korea with implications for Quaternary tectonics, Quaternary International, 199, 3-14, 2009.

Choi, K. and Kim, S. P.: Late Quaternary evolution of macrotidal Kimpo tidal flat, Kyonggi Bay, west coast of Korea, Marine Geology, 232, 17-34, 2006.

Choi, K. H.: Evolution of Coastal Dune System and Sea Level Change during Holocene in Korea, Ph.D. thesis, Seoul National University, Republic of Korea, 192 pp., 2009. (in Korean with English abstract)

Choi, K. H., Chang, T. S., Choi, J. H., Kim, Y. M., and Lee, S. Y.: Burial storm deposits recorded at the coastal dunes, Dasari, Chungnam Province, Journal of the Geological Society of Korea, 50, 539-549, 2014. (in Korean with English abstract)

Choi, S. G.: The last interglacial sea levels estimated from the morphostratigraphic comparison of the Late Pleistocene fluvial terraces in the eastern coast of Korea, The Korean Journal of Quaternary Research, 7, 1-26, 1993. (in Korean with English abstract)

Choi, S. G.: Last interglacial marine geomorphic surfaces between Gangneung to Muckho in mid-eastern coast of Korean Peninsula, Journal of the Korean Geomorphological Association, 2, 9-20, 1995a. (in Korean with English abstract)

Choi, S. G.: The comparison and chronology of the lower marine terraces in the mid-eastern coast of Korean Peninsula, Journal of the Korean Geographical Society, 30, 103-119, 1995b. (in Korean with English abstract)

Choi, S. G.: Chronological study of Late Pleistocene marine terraces around Pohang area, southeastern coast of Korea, Journal of the Korean Geomorphological Association, 3, 29-44, 1996. (in Korean with English abstract)

Choi, S. G.: Tectonic movement in the southwestern coast of the Korean Peninsula indicated by marine terraces of Soando Island, Journal of the Korean Geomorphological Association, 13, 1-10, 2006. (in Korean with English abstract)

Choi, S. G.: The estimation of the marine terrace of the Last interglacial culmination stage (MIS 5e) in the Sanhari of Ulsan coast, southeastern Korea, Journal of the Korean Geomorphological Association, 23, 47-59, 2016a. (in Korean with

685   English abstract)

Choi, S. G.: The estimation of the marine terrace of the late warm period of the Last Interglacial in the Sajin coast of Yeongdeok, southeastern coast of Korea, Journal of the Association of Korean Geographers, 5, 281-287, 2016b. (in Korean with English abstract)

Choi, S. G. and Chang, H.: Correlation and chronology of the marine terraces and thalassostatic terraces in the Yeongdeok

690   coast, south eastern Korean Peninsula, Journal of the Korean Geomorphological Association, 26, 81-96, 2019. (in Korean with English abstract)

Choi, S. G., Tamura, T., Miyauchi, T., and Tsukamoto, S.: The examination of the limitations of using the OSL dates derived from this study in the correlation of MIS 5 marine terraces distributed in the southeastern coast of the Korean Peninsula, Journal of the Korean Geomorphological Association, 25, 63-75, 2018. (in Korean with English abstract)

695   Choi, S. J.: Marine terrace of the Jinha-Ilgwang area, southeast Korea, Economic and Environmental Geology, 36, 233-242, 2003. (in Korean with English abstract)

Choi, S. J.: Marine terraces and Quaternary faults in the Homigot and the Guryongpo, SE Korea, Journal of the Petrological Society of Korea, 25, 231-240, 2016. (in Korean with English abstract)

Choi, S. J.: Review on the relative sea-level changes in the Yellow Sea during the Late Holocene, Economic and Environmental

700   Geology, 51, 463-471, 2018. (in Korean with English abstract)

Choi, S. J.: Review on marine terraces of the East Sea coast, South Korea: Gangreung – Busan, Economic and Environmental Geology, 52, 409-425, 2019. (in Korean with English abstract)

Choi, S. J., Merritts, D. J., and Ota, Y.: Elevations and ages of marine terraces and late Quaternary rock uplift in southeastern Korea, Journal of Geophysical Research: Solid Earth, 113, 1-15, 2008.

705   Chough, S. K.: Geology and Sedimentary of the Korean Peninsula, London, Elsevier, 1-363, 2013.

Chough, S. K., Lee, H. J., and Yoon, S. H.: Marine Geology of Korean Seas, Elsevier, Amsterdam, 1-313, 2000.

Chough, S. K., Lee, H. J., Chun, S. S., and Shinn, Y. J.: Depositional processes of late Quaternary sediments in the Yellow Sea: a review: Geosciences Journal, 8, 211-264, 2004.

Chun, S. S., Hwang, I. G., Ryang, W. H., Chang, T. S., Kim, J. G., and Yoon, H. H.: Western Pacific Sedimentology Meeting

710   (WPSM) Field Trip Guide Book, Sedimentology of Holocene Tidal Flats (open coast & archipelago) and Cretaceous Nonmarine (strike-slip) Basin: Gwangju, Korean Sedimentology Research Group (KSRG), 1-117, 2018.

Creveling, J. R., Mitrovica, J. X., Clark, P. U., Waelbroeck, C., and Pico, T.: Predicted bounds on peak global mean sea level during marine isotope stages 5a and 5c, Quaternary Science Reviews, 193-208, 2017.

Cummings, D. I., Dalrymple, R. W., Choi, K., and Jin, J. H.: The Tide-dominated Han River Delta, Korea, Elsevier,
715   Amsterdam, 1-376, 2016.

Dalrymple, R.W.: Tidal depositional systems, in: Facies Models 4, edited by: James, N.P. and Dalrymple, R.W., St. John's,
        Geological Association of Canada, 201-231, 2010.

Dalrymple, R. W., Zaitlin, B. A., and Boyd, R.: Estuarine facies models: conceptual basis and stratigraphic implications,
        Journal of Sedimentary Research, 62, 1130-1146, 1992.

720   Dutton, A. and Lambeck, K.: Ice volume and sea level during the last interglacial, Science, 337, 216-219, 2012.

Hong, S. C.: Constraining the Depositional Age of Marine Terrace Sediments along the Eastern Coast of Korea using Optical
        Dating, Ph.D. thesis, Seoul National University, Republic of Korea, 160 pp., 2014. (in Korean with English abstract)

Hong, S. C.: Principle and geomorphological application of rock surface luminescence dating, Journal of the Korean
        Geomorphological Association, 23, 127-136, 2016. (in Korean with English abstract)

725   Hong, S. C., Choi, J. H., Yeo, E. Y., and Kim, J. W.: Principles of K-Feldspar IRSL (InfraRed stimulated luminescence) dating
        and its applications, Journal of the Geological Society of Korea, 49, 305-324, 2013 (in Korean with English abstract)

Hong, S. H., Chang, T. S., Lee, G. S., Kim, J. C., Choi, J., and Yoo, D. G.: Late Pleistocene-Holocene sedimentary facies and
        evolution of the Jeju Strait shelf, southwest Korea, Quaternary International, 519, 156-169, 2019.

Hwang, S. I. and Yoon, S. O.: The characteristics of sedimentary facies and the geomorphological development of marine
730   terraces in Kumgok area, Youngdeok county, east coast of Korea, Journal of the Korean Geomorphological Association,
        3, 99-114, 1996. (in Korean with English abstract)

Hwang, S. I. and Yoon, S. O.: Holocene climatic characteristics in Korean Peninsula with the special reference to sea level
        changes, Journal of the Korean Geomorphological Association, 18, 235-246, 2011. (in Korean with English abstract)

Hwang, S. I. and Yoon, S. O.: The geomorphological development of marine terraces UHS (upper higher surface) and HHS
735   (high higher surface) around Yeondae-san, Gampo-Eup, southeastern coast of Korea, Journal of the Korean
        Geomorphological Association, 27, 13-28, 2020. (in Korean with English abstract)

Hwang, S. I., Shin, J. Y, and Yoon, S. O.: Marine terrace and its implications to paleoenvironment during the Quaternary at
        Suje-ri – Suryum-ri of the east coast of Gyeongju, SE Korea, Journal of the Korean Geomorphological Association, 19,
        97-108, 2012. (in Korean with English abstract)

740   Ingle, J. C. Jr.: Subsidence of the Japan Sea: stratigraphic evidence from ODP sites and onshore sections, Proceedings of the
        Ocean Drilling Program: Scientific Results 127/128 (part 2), College Station, TX, 1197-1218, 1992.

Inoue, D., Sasai, T., Yanagida, M., Choi, W. H., and Chang, C. J.: Stratigraphy of the marine terrace along the east coast in
        Korea by means of the loess-paleosol sequence and Japanese tephra, in: Abstract of the 2002 Autumn Conference of the
        Geological Society of Korea, 24-26 October 2002, 81, 2002.

745   Jin, J. H., Chough, S. K., and Ryang, W. H.: Sequence aggradation and systems tracts partitioning in the mid-eastern Yellow
        Sea: roles of glacio-eustasy, subsidence and tidal dynamics, Marine Geology, 184, 249-271, 2002.

Klein, G. D.: Intertidal flats and intertidal sand bodies, Coastal Sedimentary Environments, Springer, 187-224, 1985.

Kim, Jeong C., Ko, H. J., Lee, S. R., Lee, C. B., Choi, S. J., and Park, K. W.: 1:250,000 Geological Report of the Gangneung-Sokcho Sheets, Daejeon, Korea Institute of Geoscience and Mineral Resources, 76 pp., 2001. (in Korean with English

750   abstract)

Kim, Jin C., Chang, T. S., and Yi, S.: OSL chronology of the Huksan Mud Belt, south-eastern Yellow Sea, and its paleoenvironmental implications, Quaternary International, 503, 170-177, 2019.

Kim, J. W., Chang, H. W., Choi, J. H., Choi, K. H., and Byun, J. M.: The morphological characteristics and geochronological ages of coastal terraces of Heunghae region in northern Pohang City, Korea, Journal of the Korean Geomorphological

755   Association, 12, 103-116, 2005a. (in Korean with English abstract)

Kim, J. W., Chang, H. W., Choi, K. H., and Lee, J.: Geomorphic and Geochronologic Survey of Coastal Terraces on the East Coast of Korean Peninsula, Korea Hydro and Nuclear Power Co., Res. Rep. E03NJ07, unpublished, 1-196, 2005b. (in Korean)

Kim, J. W., Chang, H. W., Choi, J. H., Choi, K. H., and Byun, J. M.: Landform characteristics of coastal terraces and optically

760   stimulated luminescence dating on the terrace deposits in Yangnam and Yangbuk area of the Gyeongju City, South Korea, Journal of the Korean Geomorphological Association, 14, 1-14, 2007a. (in Korean with English abstract)

Kim, J. W., Chang, H. W., Choi, J. H., Choi, K. H., and Byun, J. M.: Optically stimulated luminescence dating on the marine terrace deposits of Hujeong-Jukbyeon region in Uljin, Korea, Journal of the Korean Geomorphological Association, 14, 15-27, 2007b. (in Korean with English abstract)

765 Kim, S. W.: A study on the terraces along the southeastern coast (Bang-eojin–Pohang) of the Korean Peninsula, Journal of Geological Society of Korea, 9, 89-121, 1973.

Kim, Y. H., Lee, H. J., Chun, S. S., Han, S. J., and Chough, S. K.: Holocene transgressive stratigraphy of a macrotidal flat in the southeastern Yellow Sea: Gomso Bay, Korea, Journal of Sedimentary Research, 69, 328-337, 1999.

Kopp, R. E., Simons, F. J., Mitrovica, J. X., Maloof, A. C., Oppenheimer, M.: Probabilistic assessment of sea level during the

770   last interglacial stage, Nature, 462, 863-867, 2009.

Korea Hydrographic and Oceanographic Agency (KHOA), Ocean Data in Grid Framework, www.khoa.go.kr/oceangrid/gis/category/reference/distribution.do, last access: 16 June 2021. (in Korean)

Kwon, Y. K.: Sequence Stratigraphy of the Taebaek Group (Cambrian-Ordovician), Mideast Korea and Seismic Stratigraphy of the Western South Korea Plateau, East Sea, Ph.D. thesis, Seoul National University, Republic of Korea, 205 pp., 2005.

775 Kwon, Y. K., Yoon, S. H., and Chough, S. K.: Seismic stratigraphy of the western South Korea Plateau, East Sea: implications for tectonic history and sequence development during back-arc evolution, Geo-Marine Letters, 29, 181-189, 2009.

Lee, D. Y.: Stratigraphic research of the Quaternary deposits in the Korean Peninsula, The Korean Journal of Quaternary Research, 1, 3-20, 1987.

Lee, E. and Chang, T. S.: Holocene sea level changes in the eastern Yellow Sea: a brief review using proxy records and

780   measurement data, Journal of the Korean Earth Science Society, 36, 520-532, 2015. (in Korean with English abstract)

Lee, G. R. and Park, C. S.: Properties of deposits and geomorphic formative ages on marine terraces in Gwangyang Bay, South Sea of Korea, Journal of the Korean Geographical Society, 3, 346-360, 2006. (in Korean with English abstract)

Lee, G. R. and Park, C. S.: Study on Development and Distributional Characteristics of Terrace in the West and South Coast of Korea, Kyungpook National University and Korea Institute of Geoscience and Mineral Resources, unpublished, 1-111,

785   2018. (in Korean with English abstract)

Lee, G. R. and Park, C. S.: Comparison of uplift rate in the southern coast of the Korean Peninsula, Journal of the Korean Geomorphological Association, 26, 55-67, 2019a. (in Korean with English abstract)

Lee, G. R. and Park, C. S.: Production of Uplift Rate Map in the East Coast using Studies on Marine Terraces, Kyungpook National University and Korea Institute of Geoscience and Mineral Resources, unpublished, 1-106, 2019b. (in Korean

790   with English abstract)

Lee, G. R. and Park, C. S.: Uplift rate map and distribution of uplift rate in the east coast of the Korean Peninsula, Journal of the Korean Geomorphological Association, 27, 47-60, 2020. (in Korean with English abstract)

Lee, J. Y., Kim, J. C., Lim, J., Kota, K., Hong, S. S., Moon, J. A., and Kim, Y. E.: Depositional environments and ages of coastal deposits in Gwanpo-ri, Geoje Island, Journal of the Geological Society of Korea, 49, 661-667, 2013. (in Korean

795   with English abstract)

Lee, S. Y., Seong, Y. B., Kang, H. C., Choi, K. H., and Yu, B. Y.: Cosmogenic ^{10}Be and OSL dating of marine terraces along the central-east coast of Korea: spatio-temporal variations in uplift rates, The Open Geography Journal, 7, 28-39, 2015.

Li, C., Chen, G., Yao, M., and Wang, P.: The influences of suspended-load on the sedimentation in the coastal zones and continental shelves of China, Marine Geology, 96, 341-352, 1991.

800 Li, X. S., Zhao, Y. X., Feng, Z. B., Liu, C. G., Xie, Q. H., and Zhou, Q. J.: Quaternary seismic facies of the South Yellow Sea shelf: depositional processes influenced by sea-level change and tectonic controls, Geological Journal, 51, 77-95, 2016.

Lim, D. I., Jung, H.S., Kim, B.O., Choi, J.Y., and Kim, H.N.: A buried palaeosol and late Pleistocene unconformity in coastal deposits of the eastern Yellow Sea, East Asia, Quaternary International, 121, 109-118, 2004.

Marsset, T., Xia, D., Berne, S., Liu, Z., Bourillet, J. F., and Wang, K.: Stratigraphy and sedimentary environments during the

805   Late Quaternary in the Eastern Bohai Sea (North China Platform), Marine Geology, 135, 97-114, 1996.

Mauz, B. and Bungenstock, F.: How to reconstruct trends of late Holocene relative sea level: A new approach using tidal flat clastic sediments and optical dating, Marine Geology, 237, 225-237, 2007.

Mauz, B., Vacchi, M., Green, A., Hoffmann, G., and Cooper, A.: Beachrock: a tool for reconstructing relative sea level in the far-field, Marine Geology, 362, 1-16, 2015.

810 Mayer, R. H. and Kriebel, D. L.: Wave runup on composite-slope and concave beaches, in: Proceedings of the 24th Coastal Engineering Conference, ASCE, 2325-2339, 1994.

Molnar, P. and Tapponnier, P.: Cenozoic tectonics of Asia - effects of a continental collision, Science, 189, 419-426, 1975.

Muhs, D. R., Kelsey, H. M., Miller, G. H., Kennedy, G. L., Whelan, J. F., and McInelly, G. W.: Age estimates and uplift rates for late Pleistocene marine terraces: Southern Oregon portion of the Cascadia forearc, Journal of Geophysical Research, 815   95, 6685-6698, 1990.

Murray, A. S., and Wintle, A. G.: Luminescence dating of quartz using an improved single-aliquot regenerative-dose protocol, Radiation Measurements, 32, 57-73, 2000.

Nam, S. H., Lyu, S. J., Kim, Y. H., and Kim, K.: Correction of TOPEX/POSEIDON altimeter data for nonisostatic sea level response to atmospheric pressure in the Japan/East Sea, Geophysical Research Letters, 31, L02304, 2004.

820   Nam, S. H., Park, J. H., and Park, J. J.: High-frequency variability: Basin-scale oscillations and internal waves/tides, in: Oceanography of the East Sea (Japan Sea), edited by: Chang, K.I., Zhang, C.I., Park, C., Kang, D.J., Ju, S.J., Lee, S.H., and Wimbush, M., Springer, Cham, 127-148, 2015.

National Geographic Information Institute: Korean Official Vertical Datum since 1964, https://www.ngii.go.kr/eng/content.do?sq=110, last access: 16 June 2021.

825   Oh, G. H.: The geomorphic history of the southeastern coast of the Korean Peninsula, Geographical Review of Japan, 50, 689-699, 1977. (In Japanese with English abstract)

Oh, J. S.: Discussion on the characteristics and formation age of the reddish-yellow semi-consolidation deposits, west coast of Korea: comparison with the Ujeon coast deposits in Jeungdo, Journal of the Association of Korean Geographers, 7, 55-68, 2018. (in Korean with English abstract)

830   Oh, I. S., and Lee, D. E.: Tides and tidal currents of the Yellow and East China Seas during the last 13000 years, Journal of the Korean Society of Oceanography, 33, 37-145, 1998.

Otvos, E.G.: Beach ridges – definitions and significance, Geomorphology, 32, 83-108, 2000.

Park, C. S., Kihm, Y. H., Nahm, W. H., and Lee, G. R.: Formative age of coastal terraces and uplift rate in the east coast of South Korea, Journal of the Korean Geomorphological Association, 24, 43-55, 2017. (in Korean with English abstract)

835   Park, Y. A., Lim, D. I., Khim, B. K., Choi, J. Y., and Doh, S. J.: Stratigraphy and subaerial exposure of late Quaternary tidal deposits in Haenam Bay, Korea (south-eastern Yellow Sea): Estuarine, Coastal and Shelf Science, 47, 523-533, 1998.

Pugh, D. and Woodworth, P.: Sea-Level Science: Understanding Tides, Surges, Tsunamis and Mean Sea Level, Cambridge University Press, Cambridge, 1-395, 2014.

Ren, J., Tamaki, K., Li, S., and Junxia, Z.: Late Mesozoic and Cenozoic rifting and its dynamic setting in Eastern China and 840   adjacent areas, Tectonophysics, 344, 175-205, 2002.

Rhodes, E. J.: Optically stimulated luminescence dating of sediments over the past 200,000 years, Annual Review of Earth and Planetary Sciences, 39, 461-488, 2011.

Rovere, A., Raymo, M. E., Vacchi, M., Lorscheid, T., Stocchi, P., Gomez-Pujol, L., Harris, D. L., Casella, E., O'Leary, M. J., and Hearty, P. J.: The analysis of Last Interglacial (MIS 5e) relative sea-level indicators: Reconstructing sea-level in a 845   warmer world, Earth-Science Reviews, 159, 404-427, 2016.
Rovere, A., Ryan, D., Murray-Wallace, C., Simms, A., Vacchi, M., Dutton, A., Lorscheid, T., Chutcharavan, P., Brill, D., Batz, M., Jankowski, N., Mueller, D., Cohen, K., and Gowan, E.: Descriptions of database fields for the World Atlas of Last Interglacial Shorelines (WALIS), Zonodo, https://doi.org/10.5281/zenodo.3961543, last access: 16 June 2021.

850   Ryang, W. H., Kwon, Y. K., Jin, J. H., Kim, H. T., and Lee, C. W.: Geoacoustic velocity of basement and Tertiary successions of the Okgye and Bukpyeong coast, East Sea, Journal of the Korean Earth Sciences Society, 28, 367-373, 2007. (in Korean with English abstract)

Ryang, W. H., Kwon, Y. K., Kim, S. P., Kim, D. C., and Choi, J. H.: Geoacoustic model at the DH-1 long-core site in the Korean continental margin of the East Sea, Geosciences Journal, 18, 269-279 2014.

Schellart, W. P. and Lister, G. S.: The role of the East Asian active margin in widespread extensional and strike-slip
855   deformation in East Asia, Journal of the Geological Society, 162, 959-972, 2005.

Shennan, I., Long, A. J., Horton, B. P.: Handbook of Sea-Level Research, American Geophysical Union & Wiley, Chichester, 1-581, 2015.

Shim, T. M.: Paleomagnetic Studies on the Coastal Terrace Deposits along the Youngil Bay, Eastern Coast of the Korean Peninsula, Ph.D. thesis, Yonsei University, Republic of Korea, 115 pp., 2006. (in Korean with English abstract)

860   Shin, J. Y. and Hong, S. C.: The formative processes and ages of paleo-coastal sediments in Daepo-dong Sacheon-si in the southern coast, South Korea: evaluation of the mode and rate of the late Quaternary tectonism (II), Journal of the Korean Geomorphological Association, 25, 57-70, 2018. (in Korean with English abstract)

Shin, W. J., Yang, D. Y., and Kim, J. Y.: A study on the characteristics and burial age of sediment layers at Bukpyeong myeon, Haenam gun, Journal of the Korean Geomorphological Association, 23, 41-55, 2016. (in Korean with English abstract)

865   Shin, W. J., Lee, J. H., Byun, J., and Kim, J. Y.: The evidence for the high sea level of MIS 5e and the paleo-coastal sediments from Sinji-myen, Wando-gun, Jeollanam-do, Korea, Journal of the Korean Geomorphological Association, 26, 59-78, 2019. (in Korean with English abstract)

Shinn, Y. J., Chough, S. K., Kim, J. W., and Woo, J.: Development of depositional systems in the southeastern Yellow Sea during the postglacial transgression, Marine Geology, 239, 59-82, 2007.

870   Simms, A. R.: Last interglacial sea-level proxies in the Korean Peninsula, https://zenodo.org, last access: 16 June 2021.

Song, B., Yi, S., Yu, S. Y., Nahm, W. H., Lee, J. Y., Lim, J., Kim, J. C., Yang, Z., Han, M., and Jo, K. N.: Holocene relative sea-level changes inferred from multiple proxies on the west coast of South Korea, Palaeogeography, Palaeoclimatology, Palaeoecology, 496, 268-281, 2018.

Tamaki, K., Suyehiro, K., Allan, J., Ingle J. C. Jr., and Pisciotto, K. A.: Tectonic synthesis and implications of Japan Sea ODP
875   drilling, Proceedings of the Ocean Drilling Program: Scientific Results 127/128 (part 2), College Station, TX, 1333-1348, 1992.

Thompson, S. B. and Creveling, J. R.: A global database of Marine Isotope Stage 5a and 5c marine terraces and paleoshorelines indicators, Earth System Science Data Discussions, https://doi.org/10.5194/essd-2021-14, last access: 16 June 2021.

US Army Corps of Engineers: Shore Protection Manual, Department of the Army, Waterways Experiment Station, Vicksburg,
880   Chapter 2, 1-148, 1984.

Watson, M. P., Hayward, A. B., Parkinson, D. N., and Zhang, Z. M.: Plate Tectonic History, Basin Development and Petroleum
       Source Rock Deposition Onshore China, Marine and Petroleum Geology, 4, 205-225, 1987.

Yang, D. Y., Han, M., Kim, J. C., Lim, J., Yi, S, and Kim, J. Y. Characteristics of marine terrace sediments formed during the
       Marine Isotope Stage 5e in the west south coast of the Korean Peninsula, Economic and Environmental Geology, 49,
885   417-432, 2016. (in Korean with English abstract)

Yang, J. H. Morphogenetic succession and coastal climatic terrace associated with Quaternary climatic change, southern coast
       in Korean Peninsula, Journal of the Korean Geomorphological Association, 15, 93-110, 2008. (in Korean with English
       abstract)

Yang, J. H. Holocene sea level reflected from marine terrace in Geoje Island and its influences on coastal morphogenesis,
890   Journal of the Korean Geomorphological Association, 18, 101-112, 2011. (in Korean with English abstract)

Yang, J. H., Kee, K. D., and Kim, Y. R.: Morpho-climatic milieu and morphogenetic succession of coastal terrace in Suncheon
       Bay, Journal of the Korean Geomorphological Association, 20, 57-74, 2013. (in Korean with English abstract)

Yoo, D. G., Lee, G. S., Kim, G. Y., Kang, N. K., Yi, B. Y., Kim, Y. J., Chun, J. H., and Kong, G. S.: Seismic stratigraphy and
       depositional history of late Quaternary deposits in a tide-dominated setting: An example from the eastern Yellow Sea,
895   Marine and Petroleum Geology, 73, 212-227, 2016.

Yoon, H. H., Ryang, W. H., Chun, S. S., Simms, A. R., Kim, J. C., Chang, T. S., Yoo, D. G., and Hong, S. H.: Sensitive
       responses of coastal depositional system to the decreasing rates of Holocene sea-level rise in the macrotidal coast of
       Gochang, SW Korea, Journal of Sedimentary Research, submitted, 2021.

Yoon, S. H. and Chough, S. K.: Regional strike-slip in the eastern continental margin of Korea and its tectonic implications
900   for the evolution of Ulleung Basin, East Sea (Sea of Japan), Geological Society of America Bulletin, 107, 83-97, 1995.

Yoon, S. O., Hwang, S. I., and Jung, H. K.: A geomorphological development of marine terraces around Najung-ri and Daebo-
       ri at Gampo area, southeastern coast of Korea, Journal of the Korean Geomorphological Association, 6, 99-119, 1999. (in
       Korean with English abstract)

Yoon, S. O., Hwang, S. I., and Ban, H. K.: Geomorphic development of marine terraces at Jeongdongjin-Daejin area on the
905   east coast, central part of Korean Peninsula, Journal of the Korean Geographical Society, 38, 156-172, 2003. (in Korean
       with English abstract)

Yoon, S. O., Kwak, M., and Hwang, S. I.: Geomorphic development of marine terraces around the Kangdong area, Ulsan
       metropolitan city, southeastern coast of Korea, Journal of the Korean Geomorphological Association, 21, 147-163, 2014.
       (in Korean with English abstract)

910   Yoon, S. O., Park, C. S., and Hwang, S. I.: Geomorphic development of marine terraces in the Nampo area, Boryeong-si,
       Chungnam Province, Journal of the Korean Geomorphological Association, 22, 75-87, 2015. (in Korean with English
       abstract)